Márcia Tojeira Tavares

Licenciada em Bioquímica

Development of composite particles for pulmonary delivery

Dissertação para obtenção do Grau de Mestre em

Biotecnologia

Orientadora: Prof. Doutora Ana Aguiar-Ricardo, FCT-UNL

Co-orientadora: Doutora Teresa Casimiro, FCT-UNL

Júri:

Presidente: Prof. Dr. Carlos Salgueiro

Arguente: Dr. Eunice Costa

Vogais: Prof. Dr. Ana Aguiar-Ricardo

FACULDADE DE CIÊNCIAS E TECNOLOGIA
UNIVERSIDADE NOVA DE LISBOA

Setembro 2014

Development of composite particles for pulmonary delivery

Acknowledgments

First of all I would like to thank to my supervisor Prof. Doctor Ana Aguiar-Ricardo, for giving me the opportunity to work in the Polymer Synthesis and Processing laboratory and for all the guidance and support given throughout this year. Likewise I want to thank to my co-supervisor Doctor Teresa Casimiro, whom positive and enthusiastic supervision was very important to keep me on working without giving up.

Funding from Fundação para a Ciência e Tecnologia (FC&T-Lisbon) through contracts PTDC/EQU-EQU/116097/2009 and Pest-C/EQB/LA0006/2013 is acknowledged.

I also would like to thank to Prof. Alexandra Fernandes, for giving me the opportunity to work in her laboratory and also for the guidance, and to Pedro Martins and Anna Tolmatcheva whose help and time I appreciate very much.

To my dearest thesis partner and friend, Anita Lourenço, for making the workplace an even better one with her presence, for the support, friendship and mostly patience to deal with me on a daily basis.

To Renato Cabral, who taught me so many useful things to my work, who supported me and who was always available to help with my SAA problems, and to Ana Sousa that was my partner right from the beginning and that explained to me all that I needed to know about the SAA, I thank very much for the patience and for making those 2 hour assays so much fun.

I would also like to thank Vanessa Correia and Patrícia Morgado for all the incentive, advice and friendship, you are the best work buddies.

To Rita Restani for being a great work partner, I thank the help, but mostly I thank the joy and for always making me laugh.

To all the 510/508 lab team: Sofia Silva, Dr. Vasco Bonifácio, Telma Barroso, Tiago Reis, Rita Pires, José Pinto, Raquel Viveiros, Pedro Lisboa, Carmen Montoya and Gosia Zakrzewska.

To Mrs. Maria José Carapinha, Mrs. Conceição and Mrs. Idalina for all the assistance.

To all my friends, in and outside the university campus, for the support and for the good moments that I had with all of you this last year.

At last, I have to thank my parents and grandparents for all the help and support, without you none of this would be possible.

Abstract

In this work, biocompatible and biodegradable poly(D-L-lactide-co-glycolide) (PLGA) microparticles with the potential for use as a controlled release system of vaccines and other drugs to the lung were manufactured using supercritical CO_2, through the Supercritical Assisted Atomization (SAA) technique. After performing a controlled variance in production parameters (temperature, pressure, CO_2/solution flow ratio) PLGA microparticles were characterized and later used to encapsulate active pharmaceutical ingredients (API). Bovine serum albumin (BSA) was chosen as model protein and vaccine, while sildenafil was the chosen drug to treat pulmonary artery hypertension and their effect on the particles characteristics was evaluated. All the produced formulations were characterized in relation to their morphology (Morphologi G3 and scanning electronic microscopy (SEM)), to their physical-chemical properties (X-ray diffraction (XRD, differential scanning calorimetry (DSC), Fourier transform infrared (FTIR)) and aerodynamic performance using an *in vitro* aerosolization study – Andersen cascade impactor (ACI) - to obtain data such as the fine particle fraction (FPF) and the mass median aerodynamic diameter (MMAD). Furthermore, pharmacokinetic, biodegradability and biocompatibility tests were performed in order to verify the particle suitability for inhalation. The resulting particles showed aerodynamic diameters between the 3 and 5 μm, yields up to 58% and FPF percentages rounding the 30%. Taken as a whole, the produced microparticles do present the necessary requests to make them appropriate for pulmonary delivery.

Keywords: Microparticles; Pulmonary delivery; Poly(lactic-co-glycolic acid); Supercritical Assisted Atomization.

Resumo

Neste trabalho, desenvolveram-se micropartículas de ácido poli(láctico-co-glicolídico) (PLGA) biocompatíveis e biodegradáveis com potencial uso como sistemas de libertação controlada de vacinas e outros fármacos , através da técnica de atomização assistida por CO_2 supercrítico (SAA). Depois de variar controladamente os parâmetros de produção (temperatura, pressão, rácio CO_2/solução), as micropartículas de PLGA foram caracterizadas e posteriormente utilizadas para encapsulação de princípios ativos. A albumina do soro bovino (BSA) foi escolhida como proteína e vacina modelo enquanto o sildenafil foi escolhido como o fármaco para tratar a hipertensão arterial pulmonar, e foram avaliados os efeitos de ambos nas características das partículas. Todas as formulações produzidas foram caracterizadas em relação à sua morfologia (Morphologi G3, espectroscopia eléctronica de varrimento (SEM)), às suas propriedades físico-químicas (difracção de raio-X (DRX), calorimetria diferencial de varrimento (DSC), espectroscopia de infravermelho (FTIR)) e ao seu desempenho aerodinâmico usando um estudo de aerossolização *in vitro* – Andersen cascade impactor (ACI) - para obter valores tais como fração de partículas finas (FPF) e o diâmetro aerodinâmico mediano de massa (MMAD). Para além disso, executaram-se testes farmacocinéticos, de biodegradação e de biocompatibilidade para verificar se as partículas são adequadas para inalação. As partículas obtidas mostram diâmetros aerodinâmicos entre 3 e 5 μm, rendimentos até os 58% e percentagens de FPF a rondar os 30%. Em geral, as micropartículas produzidas apresentam os requerimentos necessários que as fazem apropriadas para administração via pulmonar.

Palavras-Chave: Micropartículas; Administração pulmonar; Ácido poli(láctico-co-glicolídico); Atomização assistida por fluídos supercríticos.

Contents

Index of Figures

Index of Tables

List of Abbreviatons

ACI: Andersen cascade impactor.

API: Active pharmaceutical ingredient.

BSA:Bovine serum albumin.

Chol: Cholesterol

Da:Aerodynamic diameter.

DoE: Design of experiment

D_n50:Particle mean numeric diameter.

DPI: Dry powder inhaler

DUSA: Dosage unit sampling apparatus

D_v50:Particle mean volumetric diameter.

DSC:Differential scanning calorimetry.

EF: Emitted fraction.

EtOx: [$Pure_{G4}$EtOx]PLGA/Chol

EtOx-SDF: [$Pure_{G4}$EtOx-SDF]PLGA/Chol

FPF:Fine particle fraction.

FTIR: Fourier transform infra red.

GSD:Geometric standart deviation.

Leu: L-Leucine.

MeOx: [$Pure_{G4}$MeOx]PLGA/Chol

MeOx-SDF: [$Pure_{G4}$MeOX-SDF]PLGA/Chol.

MMAD:Mass median aerodynamic diameter.

PLGA: Poly (lactic-co-glycolic acid).

SAS:Supercritical antisolvent.

$scCO_2$:Supercritical carbon dioxide.

SDF:Sildenafil.

T_g:Glass transition temperature.

XRD:X-ray diffraction.

1. Introduction

The routes of drug administration usually reach lungs, skin and intestinal tract, since these organs have a direct contact with the exterior. Even though the oral route is simple and the most common one, it has a risk of drug decomposition by digestive system. The transdermal route is also simple, but an adsorption efficiency of drugs is generally low in this method. Injections result in high adsorption efficiency, an early effect of injected drugs' pharmacological actions, and no risk of drug decomposition by digestive organs. However, because this is an invasive method, it provokes discomfort to patients.[1]

The local application of drugs to the respiratory tract via inhalation facilitates a site specific treatment of lung diseases (asthma, chronic obstructive pulmonary disease (COPD)) with lower systemic exposure and consequently, reduced side effects. Yet again, it is also an advantageous route for systemic drug delivery since it shows a high solute permeability, due to its very thin absorption membrane (0.1-0.2 μm), to its elevated blood flow (5L/min) and to the highly vascularized alveolar epithelium constituted by a single layer of cells, which offers a large absorptive surface (80–100 m^2). All this facilitates the distribution of the molecules throughout the body.[2,3] It also has an easy administration, shows early effects of drugs' pharmacological actions and has no risk of drug decomposition.[4] The absorption of macromolecules via the pulmonary route is rapid and facilitated by the highly vascularized alveolar epithelium. Also, unlike the oral route, it is not subject to first pass metabolism which is especially important to macromolecules (i.e. peptides and proteins) that are easily degraded by enzymes.[5]

However, the short duration of drug action in the lung is considered a significant disadvantage of conventional inhalation therapy. Hence, the development of pulmonary controlled release formulations would be highly beneficial for patients suffering from lung diseases. Controlled drug release systems composed of polymeric materials with particular characteristics, such as biocompatibility and degradability, have been shown to improve the pharmacokinetic and pharmacodynamic profiles of encapsulated drugs in the lung.[1,4]

The use of dry powders as drug delivery systems has been increasingly considered as a treatment option, even though it brings out concerns related to respiratory tract anatomy, breathing pattern and particle size.[6]

Ideally, dry powders should have high dispersibility, drug stability, narrow size distribution and sustained release. Above all, there is a need to control both size and morphology of the particles since those are the characteristics that affect drug deposition. There is also a need to make sure that the particles have a physical stability in order to prevent unfavorable solid-state transitions.[7]

1.1 Vaccines

Vaccine is an antigenic preparation used to establish immunity to a disease, which when administered to humans, provides protection against such disease by the activation of T and B cells.[8] The future of vaccines extend beyond the treatment of infectious diseases and it has been already used for cancer immunotherapy, being the first cancer vaccine licensed in 2010.[9] Vaccines are responsible for a big part of the death prevention associated with numerous infection diseases every year, even though there is still a huge amount of children morbidity due to vaccine-preventable diseases.[10] This happens because those children are mostly from developing countries, and vaccines nowadays are mainly delivered via a parenteral route, which is not the most appropriate to overcome this issue. Vaccines administered parenterally require expensive cold chain transport and trained personnel, and they can induce needle-stick injuries with possible transmission of viruses.[11,12] To treat the infectious diseases that affect poor populations the vaccines should be simple, cheap, easy to produce and stable. This is all possible with pulmonary vaccination added to all the advantages for drug delivery already mentioned.[13] Above that is the fact that the lungs have gained a lot of attention given that the respiratory tract is the main entry of pathogens and also it has an extensive dendritic cell network lining the airway epithelium that facilitates a first line of defense for antigens.[14] The ideal vaccine formulation would be one delivered in a single dose, and it is known that microparticles efficiently act as immune system adjuvants by carrying antigenic materials and by depositing them in the bronchiolar region, so the exposure to the antigen can be increased.[13,15] Even though it has already been proven that the pulmonary delivery of antigens induces immunity, there are still no dry powder vaccines on the market and the major difficulty is the adaptation of the parenteral formulation for the lung safety and efficacy.[12] Despite that, there are several known pulmonary vaccines already produced for such diseases as tuberculosis[16], influenza[11], measles[17] and hepatitis B.[18]

1.2 Pulmonary Arterial Hypertension

Pulmonary Arterial Hypertension (PAH) is characterized by heavily proliferation and apoptosis resistance of vascular cells of the lung (smooth-muscle cells, fibroblasts and endothelial cells), reducing the area of small pulmonary arteries and stiffening large pulmonary arteries that have as a consequence the increase of pulmonary vascular resistance and artery pressure.[19] This condition is normally associated with connective-tissue diseases, congenital heart disease, protopulmonary disease and HIV. Its cause is not always sure, it can occur either due to genetic mutations in the bone morphogenetic protein type II receptor (BMPR-II) that will affect the growth-suppressive effect of the bone morphogenetic protein (BMP) or even because of environmental factors (drugs, toxins, viruses).[19,20] The diminishing production of endothelial nitric oxide and the increase of the phosphodiesterase type 5 (PDE5) are the main pathologic features of PAH. While the nitric oxide stimulates the production of soluble cyclic guanosine monophosphate (cGMP) - an important

vasodilator and antiproliferative pathway in the pulmonary circulation, PDE5 is responsible for its hydrolysis. Without cGMP the levels of intracellular calcium and potassium rise and lead to vasoconstriction, proliferation of smooth-muscle cells and resistance to apoptosis.[21]

PAH treatments normally use diuretics, anticoagulation, vasodilative or antiproliferative agents. Sildenafil (Figure 1.1(a)), a PDE5 inhibitor used for the treatment of erectile dysfunction, is one of the most used therapeutic options that promotes apoptosis, reduces hyperoxia-induced lung injury, and augments pulmonary capillary density. The local delivery of sildenafil using the inhalation route allows for a reduction of drug exposure and shows more effectiveness than other routes thanks to the well-ventilated parts of the lung.[22,23]

To deliver sildenafil to the lung, it should be encapsulated using a carrier in order to maintain its stability and also to have a controlled release.[4] Dendrimers are synthetic polymers with a well-defined hyperbranched three-dimensional structure constituted by several layers as represented in Figure 1.1(b). Being able to have a nanoscale size, they are excellent carriers to use in a wide range of medical applications. They have been mainly used to deliver DNA drugs into the cell through the lung, but their use has been enlarged to other type of treatments.[24,25] One example is the Polyurea (PURE) dendrimers that are biocompatible, biodegradable and "green" dendrimers whose fluorescence is very valiable for cell imaging or biosensing.[26]

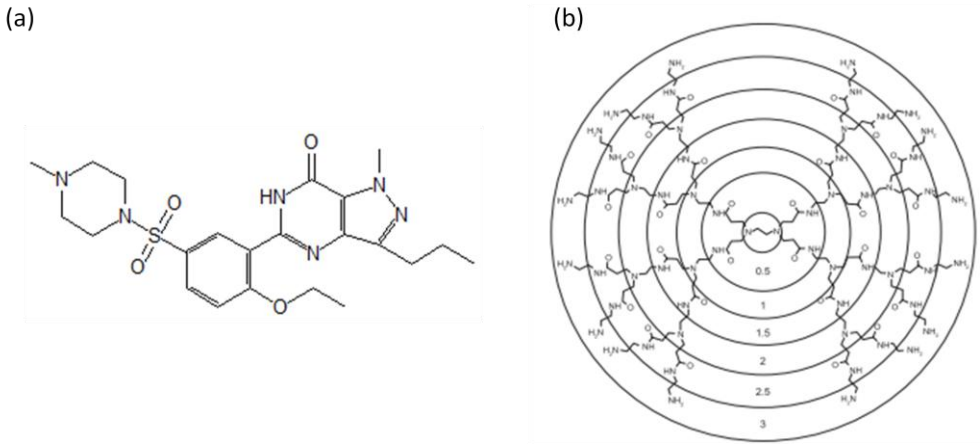

Figure 1.1 - Sildenafil (a) and a G3 Dendrimer[25] (b) structures.

The use of nanoparticles as drug release systems has been considered because of their ability to protect drugs at both extracellular and intracellular levels and then release them in a sustained and controlled manner, and especially for the fact that they are still able to penetrate into deep tissue and then suffer cellular uptake. However, nanoparticles are not in between the optimal particle size for inhalation (1-5μm) and are easily exhaled, so to improve both their aerodynamic properties and stability, they can be microencapsulated using an excipient.[27]

1.3 Dry Powder Inhalers

For it to be a good delivery device, an inhaler should generate an aerosol of a suitable size (1-5 μm) with a reproducible drug dosing that makes sure the drug chemical stability and activity are intact. Also, this device should be simple, easy to use, inexpensive and portable.[3] Taking these characteristics into account, Table 1.1 represents a comparison between the three existing inhalers.

Table 1.1 – Comparison between the different inhalers relatively to different characteristics.

	Nebulizers	**pMDI**	**DPI**
Delivery efficiency	+	-	+
Ease of use	-	-	+
Portability	-	+	+
Drug stability	-	-	+

The first inhalers to be developed and to appear on the market were the nebulizers, in which the drug is dissolved in a polar liquid. However they showed some disadvantages such as low efficiency and reproducibility, the required time to the administration was about 30 minutes and their use was confined to hospitals or home, given that they were not portable.[2,3]

To surpass these issues, the pressurized metered dose inhalers (pMDIs) were developed since they show greater efficiency and reproducibility, they are faster to use and also portable. Despite that, they also show some drawbacks since they require the use of compressed volatile liquids as propellants (i.e. chlorofluorocarbon), making them environmentally unfriendly, and because they deliver the dose at high velocity it facilitates the deposition in the oropharynx.[28]

In order to overpass these problems, the inhalers were improved, and dry powder inhalers (DPIs) appeared (Figure 1.2). Besides being easy to use and portable, they are also propellant-free, making them environmentally friendly. Also, since the aerosols are in a dry state they assure the stability of the drug, needing no special condition storage and distribution.[29] As for the delivery of vaccines these devices are very suitable once macromolecules (polysaccharides, proteins and peptides) tend to degrade when in a liquid solution and so are provided with a greater stability. That was proven by the production of a dry powder influenza vaccine by spray-freeze drying that showed an increase of the systemic and mucosal humoral and cell-mediated immune response in mice when compared with liquid vaccines.[11]

However, they are expensive, complex to develop and the uniformity of the doses depends on the patient's inspiratory flow because that is what set the particles in motion, provoking turbulence and shear in order to generate the aerosol. The particles then enter the patients airways and are carried to the deep lung.[30] These devices are divided in "single-dose" DPIs, which use a single dose capsule, in "multiple unit dose" DPIs, which contains small doses separated in several capsules or blisters and in "multidose" DPIs that contain an amount of powder that is then delivered in several metered doses.[31]

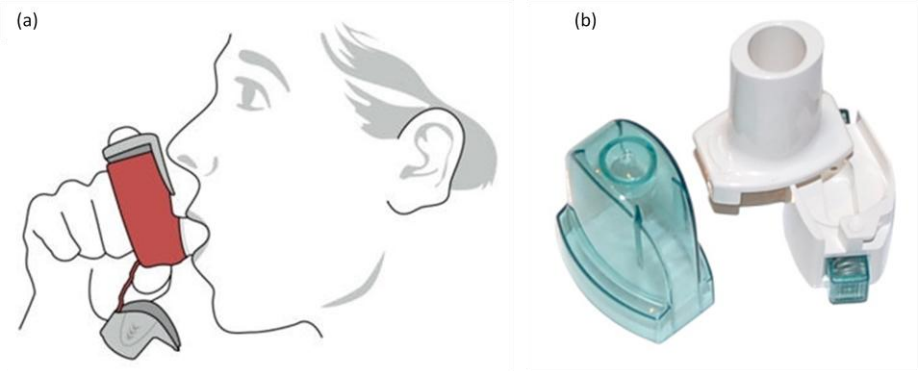

Figure 1.2 - Schematic representation of (a) a person using an inhaler [32] and (b)an example of a dry powder inhaler.[33]

1.4 Characterization of inhaled particles

In order to understand where particles with different size deposit in the respiratory tract, the aerodynamic diameter (d_a) it has to be taken into account and is defined by the equation (1)

$$d_a = d_g\sqrt{\frac{\rho_p}{\rho_o x}} \quad (1)$$

Where ρ is the mass density of the particle, ρ_o is the unit density and x the particle dynamic shape factor.[2]

Though some conflicts regarding the range for optimal d_a to efficiently reach the deep lungs may exist, the most recent works states that the aerodynamic diameter of aerosol particles should be between 1 and 5 μm since these size range is the one that gets to the deep lungs (Figure 1.3). While smaller particles may fail to deposit and are exhaled, bigger ones may accumulate in the mouth and throat by inertial impaction. The particles in between should deposit in the deep lung by inertial impaction and sedimentation.[34–36]

Moreover, smaller particles are more likely phagocytized and have the tendency to aggregate due to van der Waals and electrostatic forces[37], making large porous particles with low density suitable for lung delivery.[38] Large porous particles have a mean diameter bigger than 5 μm and an associated low mass density, so even though these particles have large geometric diameters, they exhibit aerodynamic diameters comparable to smaller particles due to their low density. Since they have large sizes, these particles will avoid clearance by alveolar macrophages, enabling sustained drug delivery through the lungs. Furthermore, increasing the geometric diameters would increase the dispersibility and entrainment of the drug particles from the inhaler and finally they would tend to de-aggregate much easier than small non-porous particles.[5,7]

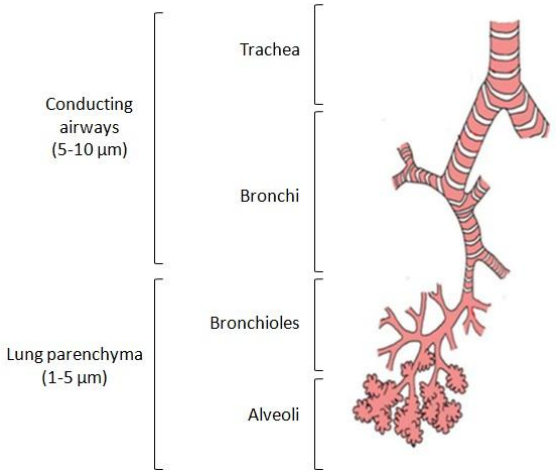

Figure 1.3 - Representation of the different stages of the respiractory tract and the particles' deposition according to size. Adapted from Ungaro F. *et al.*[39]

The mass median aerodynamic diameter (MMAD) is the particle diameter that can be obtained with the use of an *in vitro* aerosolization study such as a multistage cascade impactor, and it corresponds to 50% of the cumulative distribution. With the same apparatus it is possible to calculate the fine particle fraction (FPF) that is the mass of particles under a cut-off diameter of around 5 µm and with the use of a dosage unit sampling apparatus (DUSA) the shot weight can be determined, which is the proportion of powder that exits the capsule.[40]

In regards to inhaler products' testing, the Andersen cascade impactor (ACI) and the next generation impactor (NGI) are the recommended by both the European and US pharmacopeia, since the airflow and differential pressure over the inhaler are easily controlled.[41,42] ACI is a sizing sampler containing 8 aluminium stages, each with a collection plate and a filter, and an induction port with a suitable mouth piece adapter. At times a pre-separator is used to collect large masses of non-respirable powders. The air flow rate should provide a pressure drop of 4 KPa with a defined time that allows the passage of 4 liters of air through the ACI. The inhaled aerosol will be fractionated into different stages that have a decrease in the nozzles' diameter throughout the apparatus as represented in Figure 1.4. The particles deposition on each collection plate will depend on their size and density, and subsequently their inertia, being the particles with larger d_a collected in the early stages and the smaller ones on the last.[41,43]

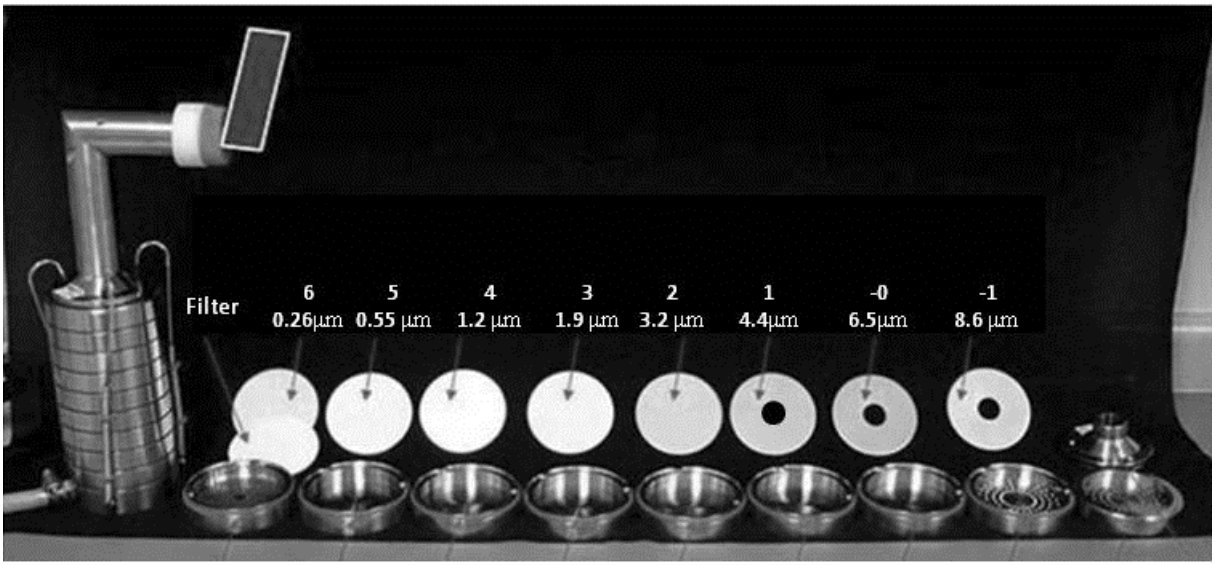

Figure 1.4 - Representation of the Andersen cascade impactor as well as its different stages and respective cut-off diameters at 60 L/min, adapted from Mitchell, J. P. *et al.*[44]

In order to provide a sustained controlled release, drug-polymer systems were produced and because of that the release of the drug is dependent not only in the diffusion rate from the non-degraded polymer, but also by its swelling and erosion.

By modeling the drug release using mathematical equations, important information regarding mass transport and chemical processes relatively to the drug delivery system can be acquired, coupled with the effect of the parameters, for instance particle geometry or drug loading.[45]

When it comes to model the drug release out of polymeric matrices, the Korsmeyer-Peppas equation (2) has been the most used one, even though it stands on a simple method to study only the importance of the diffusional exponent, n, which indicates the transport mechanism. The mechanism can either be due to the Fickian diffusional release (n=0.43) or polymer's swelling (n=0.85). It also considers a *k* that is a constant incorporating characteristics of the macromolecular network system of the drug.[46] However, it is only valid to the first 60% of the release, because the further release is dependent on other factors that are not taken into account, such as particles degradation.

$$\frac{M_t}{M_\infty} = \mathrm{k}t^n \quad (2)$$

Notwithstanding, taking the Peppas and Sahlin equation (3) in consideration, two competing release mechanisms are taken into account: Fickian diffusional release and the Case-II relaxation release that corresponds to the second part of the equation. This mechanism is present when the release of the drug is due to stresses and state-transition in hydrophilic glassy polymers that suffer swelling when in contact with liquid solutions such as body fluids.[47]

$$\frac{M_t}{M_\infty} = K_d t^m + K_r t^{2m} \quad (3)$$

The m is equally a Fickian diffusion exponent and equals n when the relaxation mechanism is not present while both K_d and K_r are constants. Using this model all the 100% of the drug can be acknowledged.

Another important characteristic of the pharmaceuticals is its solid-state chemistry, in view of the fact that the existing polymorphism of the particles will have an influence on the stability of the drug and on the flowability as well. For lung delivery particles, the carrier should be amorphous because it brings out increased dissolution rates, higher water adsorption and also it is crucial for storage purposes while the API is preferably crystalline so the bioavailability is maintained. Nonetheless, and contrarily to crystalline forms, amorphous compounds are defined by a disorder arrangement of its molecules, showing less stability and more reactivity.[30,48] For that, it is important to access to a particle engineering process where these characteristics can be controlled. The most used technique to evaluate the solid-state is the X-ray Diffraction (XRD), which is based on the long-range order present, defining the intermolecular spacing of the unit cell and giving subsequently the crystalline system.[49]

In order to better understand a process and to reach full efficiency, knowledge at a theoretical level is advantageous, especially with the application of a statistical method like design of experiment (DoE). DoE is useful to obtain precise data and information of a process without the need of a large amount of experiments and associated costs. For instance, using a fractional factorial design it is possible to test parameters based on the obtained results and perform a screening. On the other hand, by performing a full factorial design the variables interaction can be studied. This kind of study is performed by an analysis of variance (ANOVA), which is going to test whether the difference between groups' means are significant or not by comparing variances of the distributions. Basically, the variances are tested for statistical significance, and if significant the null hypotheses (all the groups are considered the same) is rejected and it is possible to admit that the means are different from each other.[50]

1.5 Poly (lactic-co-glycolic acid)

Poly (lactic-co-glycolic acid) (PLGA) (Figure 1.5) is used as a biodegradable slow-release polymer, it is physically strong, highly biocompatible and bioabsorbable and also allows an effective encapsulation of all kinds of drugs, proteins and various other macromolecules such as DNA, RNA and peptides.[51,52] Additionally, it was approved by the FDA (Food and Drug Administration) for drug targeting in the year 2000, being one of the first among all the new minimally invasive protein delivery system options, which makes it one of the most promising materials in medical and biotechnological research with high commercial interest.[53,54] PLGA has been the focus of extensive

research for release of therapeutic proteins and it is the most popular among the various available biodegradable polymers because of its long clinical experience, favorable degradation characteristics, bioadhesive properties and possibilities for sustained drug delivery.[51,53]

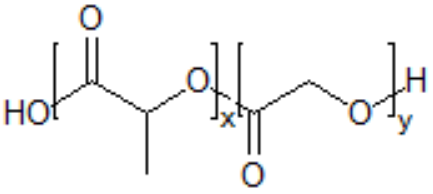

Figure 1.5 - PLGA structure, with the lactic acid between the left-side brackets and the glycolic acid between the right-side brackets. x and y represent the number of times the unit it repeated.

A main influence on the release is the polymer biodegradation. PLGA's ester backbone undergoes hydrolysis in aqueous environments, such as body fluids, and the polymer eventually degrades to lactic and glycolic acid monomers with well-established compatibility and safety profile since the products are nontoxic, noncarcinogenic, and nonteratogenic.[54–56] Lactic acid is converted to pyruvate, which is degraded in the Krebs cycle via acetylating of coenzyme A, and carbon dioxide, which is mainly eliminated by respiration. Part of the glycolate is excreted directly via the urine while another part is oxidized to glyoxylate, which is converted to glycine, serine and pyruvate.[53]

The presence of a drug may change the mechanism from bulk erosion to surface degradation. In general, the PLGA degradation and the drug release rate can be accelerated by greater hydrophilicity, increase in chemical interactions among the hydrolytic groups, less crystallinity and larger volume to surface ratio of the particles. In spite of that, higher content of glycolic acid leads to quicker rates of degradation with an exception of 50:50 ratio of PLA/PGA, which exhibits the fastest degradation.[51]

The T_g (glass transition temperature) of the PLGA copolymers are reported to be above the physiological temperature of 37 ºC and hence are glassy in nature, exhibiting fairly rigid chain structure. It is known that the T_g decrease with a decrease of lactide content in the copolymer composition and with a decrease in molecular weight.[51] The glass transition temperature for 50:50 ratio is between 45 and 50 ºC. [55]

As for the risk of inflammation *in situ* caused by the polymer, there is some discrepancy in the literature as to whether that is true or not. Some groups suggest PLGA particles are inflammatory *in vitro* and *in vivo*[57], whereas others have not found this to be the case.[58,59] The discrepancy between these findings may be due to differences in particle fabrication or experimental settings. However, given the long clinical history of PLGA and the broad literature reporting PLGA particle uses for biomedical applications, it seems unlikely that particles derived from PLGA would trigger potent inflammatory responses.[58]

When the delivery of small proteins and peptides is needed, the production of PLGA particles has reduced multiple injections to once every one to three months. During this incubation time, large

globular proteins must remain encapsulated at the physiological temperature, and in the dry powder state the retention of their structural integrity and biological activity is successful.[8] Moreover, the majority of proteins and peptides are hydrophilic and any attempt to load them into hydrophobic PLGA becomes a challenging task, because most methods developed often require the use of aqueous media.[8]

For vaccination purposes, antigen is mostly formulated in PLGA microparticles that are ingested by phagocytic cells following administration, resulting in particle degradation and antigen presentation.[52] Also, the use of this polymer allows the possibility of the development of a single-dose vaccine due to the controlled particle degradation to several weeks.[13]

1.6 Bulking Agents

In order to obtain particles with the ideal characteristics for lung delivery it is sometimes required the use of bulking agents and dispersibility enhancers. Ideally, bulking agents will cover the particles during their formation, keeping them from agglomerating in the drying process and also during the storage[60], hence decreasing the bulk density and increasing the dispersibility.[61] One the most used in the literature is L-Leucine (Figure 1.6 (a)), a nontoxic and nonirritant amino acid, known to improve flowability and dispersibility.[62] It was proved that the addition of leucine improved FPF given that it reduced the cohesiveness and coalescence of the particles.[37]

Another option is the use of cholesterol (Figure 1.6 (b)), a neutral lipid that because of its hydrophobic nature reduces the absorption of the ubiquitous vapor leading to a reduction in the aggregation and the adhesion of particles. Besides, it is biocompatible and it is easily metabolized, being cleared out by direct absorption by either epithelial cells or by macrophage uptake.[63]

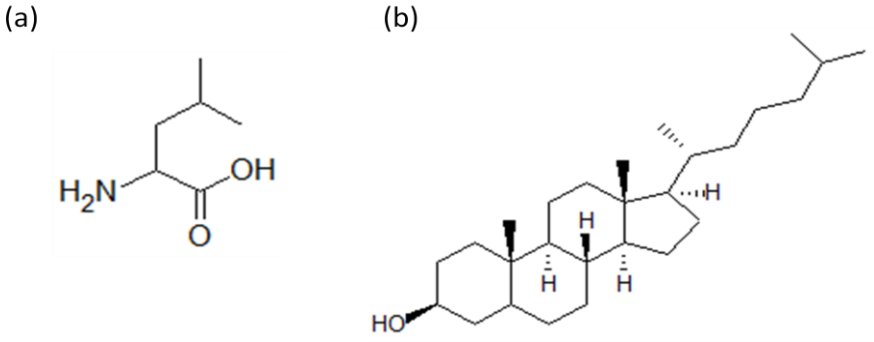

Figure 1.6 - L-leucine (a) and cholesterol (b) structures.

1.7 Particle Production

There are several known methods to produce particles for inhalation and those can be divided into two groups: the top-down (large particles are mechanically broken down to smaller ones) and the bottom-up (particles are formed from the molecular level).

Milling is based on a top down approach since it consists on the grinding of bulk crystallized particles into small ones with the use of mechanical forces such as pressure, friction, attrition, impact or shear.[25] In order to produce particles for inhalation, there are three types of mills that can be used, fluid-energy mills (jet-milling), high-peripheral-speed mills (pin-mill) and ball mills. The most used technique is jet-milling where high-pressure nitrogen is used to provide a sonic velocity to solid particles, which makes them collide and fracture into particle down to 1μm. Even though it is considered a traditional particle production technique with a low cost associated, it is inadequate when it comes to particle production since the control of size distribution is limited.[64] Also the process might change the physicochemical properties of the material, turning the surface of fractured crystals amorphous.[31]

The bottom-up processes tend to be more sophisticated and complex, and produce particles with a better control of its characteristics. In this case, the manufacturing methods involve the use of an antisolvent or are based on solvent evaporation as is spray-drying, the most used and studied solvent evaporation technique.[65] Spray drying is very rapid, convenient and has very few processing parameters, making it suitable for industrial scalable processing and it also provides stability and biological activity for the API. In this process, drug/protein/peptide loaded microspheres are prepared by the means of an atomization of the feed solution into a spray, which later enters in contact with heated air in a drying chamber forming a dry powder. The nature of solvent used, temperature of the solvent evaporation and feed rate affect the morphology of the microspheres. The disadvantages of this process is the adhesion of the microparticles to the inner walls of the spray-dryer, turning the yields insufficient, and the possible degradation of heat-sensitive drugs.[66,67]

1.8 Supercritical Fluid Technology

More recently, alternative particle production methods using supercritical fluids, especially supercritical CO_2 ($scCO_2$), have been proposed to overcome some limitations. Conventional methods usually require large amounts of organic solvents and thus require additional extensive purification steps to remove the residual solvent. When it comes to using $scCO_2$, organic solvents can be minimized or eliminated easily, since $scCO_2$ has a high affinity for them which enables their removal. A rapid expansion of the CO_2 using a pressure drop leads to the clustering of CO_2 molecules inside the liquid polymer, expanding it and inducing pore formation, making the system suitable for drug deliver.[5,51] Moreover, the morphology and porosity can be easily altered by changing operation parameters such as pressure, temperature and gas release rate.[68]

Supercritical Fluids (SF) are gases or liquids that are above their critical temperature and pressure, and that present characteristics of both states. In one hand they have the density of a liquid, which shows advantageous solvation power, while in the other hand they have the viscosity of a gas with an associated high diffusivity. Since these aspects are very changeable near the critical point, it is easy to control both of them by a slight change in pressure/temperature.[69] Also, near the critical point the compressibility and the heat capacity are much higher than in other conditions.

Carbon dioxide is the most used gas as a SF, since it is nontoxic, nonflammable, inexpensive and readily available in high purity from a variety of sources. Because it is a gas at normal pressure by simply reducing the pressure of the system, it is possible to easily separate the solvent and residues from the polymer, leading to highly pure materials.[70,71] Besides, it has a low critical point (31.1°C/73.8 bar)(Figure 1.7), which is suitable to use with heat-sensitive materials and can reduce manufacturing complexity and energy.[72]

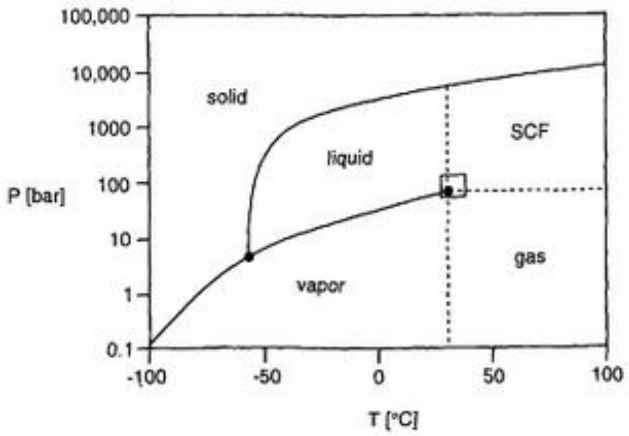

Figure 1.7 - Phase diagram of CO_2 adapted from Leitner W. et al.[73]

There are several particle production techniques that use supercritical fluids, such as supercritical fluid extraction where particles are produced when a solution is brought into contact with $scCO_2$ in a semi-continuous method[74,75], rapid expansion of supercritical solutions (RESS) where the solid material is dissolved in $scCO_2$ and the solution is expanded by depressurization, leading to a fast decrease of temperature that will induce supersaturation and consequently microparticle formation[48,76] and particles from gas saturated solutions (PGSS)[77,78] that consists in two steps: the saturation of a solution with CO_2 and the mixture's expansion through a nozzle into a spray tower.

1.9 Supercritical Assisted Atomization

Supercritical assisted atomization is proposed and patented by E. Reverchon in US 7276190B2[79] to overcome some of the problems associated with other SF techniques, for instance, some antisolvent precipitation processes (e.g. SAS) cannot be used with water-soluble compounds or the fact that RESS requires a big amount of CO_2 with low productivity.[80]

SAA is based on the solubility of controlled quantities of $scCO_2$ in a liquid solution containing the drug and excipient. The mixing happens in a heated saturator with a large contacting surface, assuring a high residence time and a near-equilibrium solubilization of the CO_2. The gaseous properties of $scCO_2$ allow it to diffuse into the amorphous regions of polymers where it enters into the free volume between the individual chains. The chain separation increases, enhancing the mobility as a result and inducing a proper mixing. This lowers the T_g of amorphous polymers, enabling them to be liquefied and since it is reversible, the T_g returns to the original value upon the complete removal of the $scCO_2$. The solution is atomized through a nozzle (thin-wall injector) into a precipitator in the form of a spray. The CO_2 works as a cosolute, since it dissolves itself in the liquid solution and it also works as a pneumatic agent, atomizing the solution in fine droplets (pneumatic atomization). After that there is a second atomization due to the CO_2 expansion existing in the fine droplets interior (decompressive atomization) (Figure 1.8).[56,81]

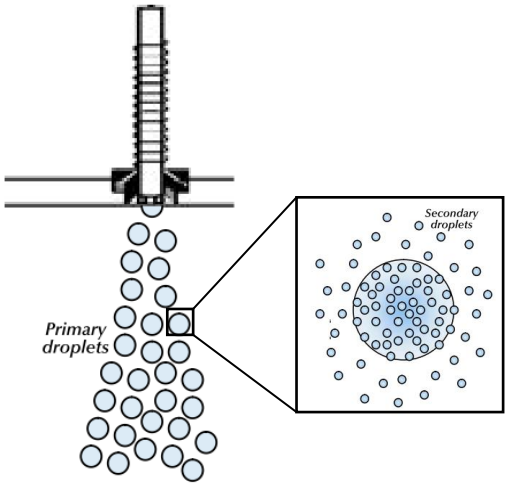

Figure 1.8 - Representation of SAA's double atomization: pneumatic atomization (left-side) and decompressive atomization (right side), adapted from Porta, G. Della *et al.*[81]

One important factor to keep in mind is the full solubilization of the $scCO_2$ in the liquid solution, and that is going to depend on such factors as the pressure and temperature because those are related to the high–pressure vapor liquid equilibria (VLE). Moreover, the presence of the solute might also induce some modifications and that has to be taken into account because in order to have a successful atomization a single-phase should be formed in the saturator.[82,81] Nonetheless, when one is working with a complicated ternary mixture it is known that by using high pressure and temperature, it becomes easier to avoid a two-phase behavior.[83] Another problem is the use of aqueous solutions due to the low solubilization of CO_2 in water, but that can be resolved with the use of an organic solvent and the reduction of water percentage to a minimum.[82]

In this work composite particles using PLGA as an excipient were produced using SAA. In one hand BSA was used as a model antigen for security reasons, and L-leucine as a bulking agent in order to develop pulmonary vaccines. In the other hand sildenafil-loaded dendrimers were encapsulated to produce nano-in-micro particles to treat pulmonary hypertension using cholesterol as a bulking agent. Furthermore all the particles were properly characterized to make sure they were suitable for pulmonary delivery.

2. Experimental Section

2.1 Materials

Poly(D-L-lactide-co-glycolide) (PLGA, PURASORB® PDLG 5002A, molar ratio: 50/50, inherent viscosity 0.21dl/g) was purchased from PURAC (Gorinchem, Netherlands). Bovine Serum Albumin (BSA, Mw 60 kDa), L-Leucine (>98%), cholesterol (94%), acetone (99.8%) and acetonitrile were obtained from Sigma-Aldrich. Ethanol (96%) was purchased in Panreac. The sildenafil-loaded dendrimers were developed in the host laboratory[1]. Industrial carbon dioxide (purity ≥ 99.93%) was obtained from Air Liquide.

2.2 Microparticles Preparation

2.2.1 BSA-Loaded Microparticles

A solution of 0.47% (w/v) PLGA, 0.09% (w/v) BSA and 0.02% (w/v) L-Leucine was prepared with 83% (v/v) acetonitrile and 16% (v/v) distilled water. While the PLGA was dissolved in part of the acetonitrile, both the BSA and Leucine were dissolved in water. After full dissolution the aqueous solution was added to the PLGA solution under stirring, with the rest of the acetonitrile added in the end.

2.2.2 SDF-Loaded Dendrimers Encapsulated in Microparticles

A solution of 0.28% (w/v) PLGA, 0.19% (w/v) cholesterol and 0.14% (w/v) sildenafil-loaded dendrimers was prepared with 42.3% (v/v) acetonitrile and 39.5% (v/v) acetone and 18.3% (v/v) ethanol. The PLGA was previously dissolved in acetonitrile, the cholesterol in acetone and the sildenafil-loaded dendrimers in ethanol.

2.2.3 SAA Apparatus

The laboratory scale SAA apparatus, represented in Figure 2.1 consists of two high-pressure pumps to deliver the liquid solution (HPLC pump 305 Gilson) and the CO_2 (HPLC pump K-501, Knauer) to the static mixer. Since the CO_2 pump is suitable for liquid solutions, there is a need to liquefy the CO_2 in a cryogenic bath. Before entering the static mixer the CO_2 is heated in an oil bath. The static mixer (3/16 model 37-03-075 Chemieer) is a high-pressure vessel with a 4.8 mm diameter, 191 mm length and 27 helical mixing elements that allows the solubilization of the CO_2 into the liquid solution due to its high surface packing. In order to control the temperature of the mixture, the static mixer is enrolled by heating tapes controlled by a shinko FCS-13A temperature controller (0.2^{o}C resolution). The obtained mixture is then atomized into the precipitator in the form of a spray by the passage through a nozzle with an internal diameter of 150 μm. At the same time, a flow of previously heated compressed air enters the precipitator to evaporate the liquid solvent. The visual recipitator is an aluminium vessel that operates at near-atmospheric conditions heated by a set of heating tapes that are connected to a

Setra pressure indicator (0.1 psig stability). To indicate the pressure of the precipitator an EROELECTRONIC LDS controller (0.1°C stability) is connected to the top of it. After the precipitator there is a heating tape set to make sure the flow remains at high temperatures, thus avoiding heat losses and consequent solvent condensation, connected to an Isopad TD 2000 heat controller (0.1°C stability). The particles will then be collected from a filter (FSI, nylon mono-filament, 1 μm) which is placed in a cyclone that helps with the separation between the particles and the CO_2-solvent flow.

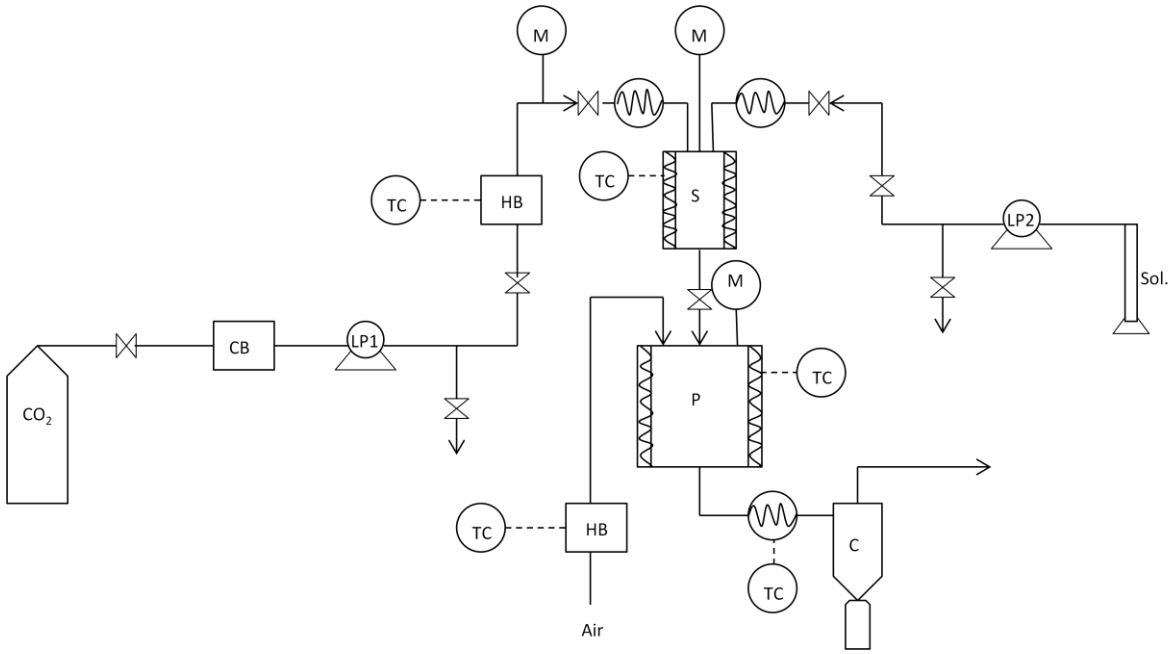

Figure 2.1 – Schematic representation of the SAA apparatus: (CB) cryogenic bath; (LP) liquid pump; (HB) heating bath; (TC) temperatute controller; (M) manometer; (S) saturator; (P) precipitator; (c) cyclone.

2.3 Microparticles Characterization

2.3.1 Particle size distribution

The particle size (PS) and the particle size distribution (PSD) were measured by a Morphologi G3 essentials, a particle analyzer system. In each particle size calculation around 30000 particles were considered. Also the span was calculated, a measure of the width of particle distribution, and it considers the $d_{v,10}$, $d_{v,50}$ and $d_{v,90}$ (particle diameter in volume corresponding to 10, 50 and 90% of the population) as represented in equation 4:

$$\text{Span}=\frac{d_{v,90}-d_{v,10}}{d_{v,50}} \qquad (4)$$

2.3.2 Particles morphology

The morphology of the produced particles was studied by Scanning Electron Microscopy (SEM) equipment from Hitachi, S-2400 instrument, with an accelerating voltage set to 15kV and at

magnifications of 5K and 10K. All the samples were dispersed on carbon tape previously attached to an aluminum stub and were coated with gold before analysis.

2.3.3 Bulk density

Once inside the calibrated cell the powder was maintained 24 h under vacuum to totally dry and degas the sample. The cell was then installed into the adsorption apparatus from the adsorption laboratory (Faculty of Sciences, University of Lisbon). Bulk density of the microparticles was determined by measuring the pressure change of helium in a calibrated volume.

2.3.4 Differential scanning calorimetry (DSC)

The differential scanning calorimetry patterns were obtained by treating the samples in a differential scanning calorimeter PerkinElmer DSC 7. The samples (10-30 mg) were placed in a holder where the temperature was raised from 25^{o}C to 300^{o}C in a heating rate of 10^{o}C/min in nitrogen.

2.3.5 X-ray diffraction

X-ray diffraction patterns were obtained by treating the samples in a RIGAKU X-ray diffractometer, model Miniflex II. Samples were placed in a holder and analyzed through CuKα radiation (3 KV/15 mA), with a 2θ angle ranging between 2^{o} and 55^{o} with a scan rate of 1^{o}/min.

2.3.6 Fourier Transform Infra Red (FT-IR)

FT-IR spectra were carried out on a PerkinElmer spectrum 1000 FTIR coupled with Opus Spectroscopy Software with potassium bromide (KBr) tablets containing 20% sample.

2.3.7 Water Content Determination

Karl Fischer coulometric titration was used for the determination of water content on the samples. An aliquot of the samples was transferred into the titration vessel and titrated with Karl Fischer reagent, which reacts quantitatively and selectively with water. The instrument was composed by the 831 KF Coulometer and a 728 stirrer both from Metrohm and by a Pt /-20…70 ºC electrode.

2.3.8 Drug Loading and Encapsulation Efficiency

The drug encapsulation was determined by milling a fixed amount of powder and then adding a known amount of PBS. The solution was under stirring for 2 h and then was centrifuged at 15000 rpm for 5 min. The supernatant was collected and the amount of drug was obtained by UV spectroscopy. The percentage of encapsulation was calculated from the obtained mass (m_r) and the initial mass (m_i) as represented in equation 5.

$$E(\%)=\frac{m_r}{m_i} \quad (5)$$

2.3.9 Aerodynamic Properties

2.3.9.1 Emitted Fraction

To determine the shot weight, which is the amount of powder that is released from the capsules, the Dosage Unit Sampling Apparatus (DUSA) is used. The air is drawn by a High Controller Pump model HCP5 (Copley) that simulates inhalation and air flow was regulated in a Critical Flow Controller model TPK (Copley) until the P1 pressure achieves the 4kPa. The air flow (Q_{air}) was measured with a flow meter model DFM3 (Copley) in order to calculate the run time of each capsule using the equation 6:

$$t(s)=\frac{4L}{Q_{air}\,(L/min)} \text{ x } 60 \text{ (s/min)} \quad (6)$$

Also, there is a need to ensure that P3/P2 ≤ 0.5 in order to guarantee the critical flow.

The assay consists on the release of 4 capsules (HPMC capsules nº3 Aerovaus) with 30±2 mg of powder each from a dry powder inhaler (Plastique 60LPM – Mode 7) and it is performed in triplicate as reported in the European Pharmacopeia.[41]

The emitted fraction (%) uses the weights (mg) of the capsule before and after the assay (m_{full} and m_{empty} respectively) as represented in equation 7:

$$EF(\%)=\frac{m_{full}-m_{empty}}{m_{full}} \text{ x } 100\% \quad (7)$$

2.3.9.2 Andersen Cascade Impactor

The aerodynamic properties of fine particles were carried out using an aluminum Andersen Cascade Impactor apparatus (ACI)(Copley) (Figure 2.2). The assay is performed with the same instruments as the emitted fraction test, being the capsules prepared equally and the run time calculated using the same European Pharmacopeia protocol.[41]

The assays were performed gravimetrically, so glass microfiber filters (80mm, Filter Lab) were placed in all the stages and were weighted before and after the capsules release. In order to obtain the drug concentration on each stage, the powder of each filter was then dissolved, the solution was centrifuged and its absorbance was read in an UV spectrophotometer (PerkinElmer Lambda 35). Each capsule was drawn through the induction port into the ACI at a flow rate of 62±2 L/min for 3.9±0.2 seconds. The effective cut-off aerodynamic diameter for each stage of the ACI were: stage -1, 8.6 μm; stage -0, 6.5 μm; stage 1, 4.4 μm; stage 2, 3.2 μm; stage 3, 1.9 μm; stage 4, 1.2 μm; stage 5, 0.55 μm; stage 6, 0.26 μm.

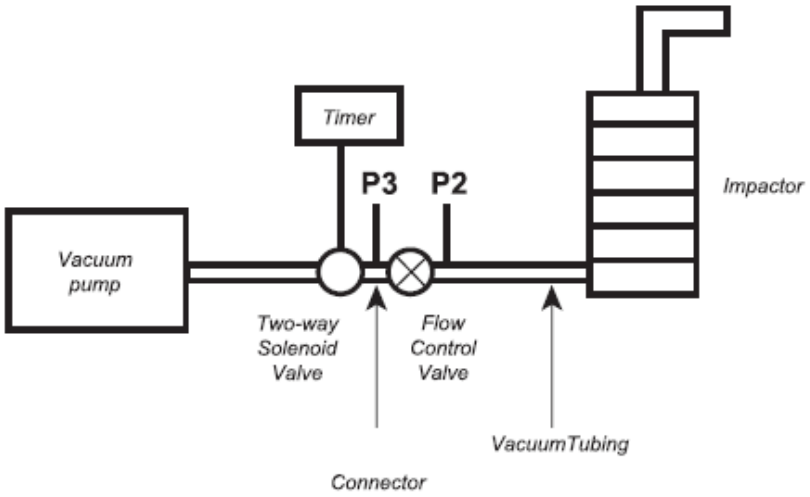

Figure 2.2 - Experimental set-up to perform ACI (adapted from European Pharmacopeia)[41].

The fine particle fraction (FPF) was determined by the interpolation of the percentage of the particles containing less than 5 μm. The Mass Median Aerodynamic Diameter (MMAD) was determined as the particle diameter corresponding to 50% of the cumulative distribution. The Geometric Standard Deviation (GSD) was determined using the values of d_{84} and d_{16}, which represent the diameters of 84% and 16% of the cumulative distribution as in equation 8:

$$GSD = \frac{d_{84}}{d_{16}} \quad (8)$$

2.3.10 Pharmacokinetic Studies

2.3.10.1 BSA-Loaded Particles

The *in vitro* release studies were carried out in phosphate-buffered saline at pH 7.4 (PBS). 60±2 mg of sample was introduced in a cellulose ester dialysis membrane (MWCO 100,000, 24 mm x 15 feet dry diameter, 1.8 mL/cm, Spectrum Labs) that was suspended in 5 mL of PBS. Samples of 0.5 mL were taken at predetermined time points and other 0.5 mL of PBS were added to the suspension and the samples.

2.3.10.2 Dendrimer-Loaded Particles

The *in vitro* release studies were carried out in phosphate-buffered saline at pH 7.4 (PBS). 20±2 mg of sample was introduced in a SnakeSkin Dialysis Tubing (3.500 MWCO, 22 mm x 35 feet dry diameter, 34 mm dry flat width, 3.7 mL/cm, Thermo Scientific) that was suspended in 10 mL. Samples of 1 mL were taken at predetermined time points and other 1 mL of PBS was added to the suspension and the samples.

The drug concentration was obtained by UV-visible spectroscopy and the drug-release profiles (%) were represented as a function of time.

The release profiles were modulated using Korsmeyer-Peppas (2) and Peppas and Sahlin (3) equations.

2.3.11 Biodegradability Assays

Biodegradation of microparticles was carried out in the presence of 0.2 mg/mL of lysozyme dissolved in PBS 10 mM at 37 ^{o}C. 2 mg of microparticles were incubated with 1 mL of lysozyme solution under horizontal agitation at 50 rpm. The enzymatic degradation medium was changed every 48 h to restore the original level of enzymatic activity. The solution was centrifuged at 13500 rpm for 7 min and the supernatant removed. Then the particles were lyophilized and weighed and the process repeated. The biodegradation rate is represented as a percentage of the remained weight (W_r) and it is calculated with the use of equation 9 where W_0 and the W_f are the initial and final particles' weight, respectively:

$$Wr(\%) = 100 - \frac{W_0 - W_f}{W_0} \times 100 \quad (9)$$

2.3.12 Biocompatibility Assays

In vitro cytotoxicity assays were performed for each cell line available and for each compound mentioned above, through the use of purity ≥ 99.93% CellTiter 96® AQueous Non-Radioactive Cell Proliferation Assay (Promega, Madison, USA), a colorimetric method for determining the number of viable cells.

At 80 % confluence, cells were harvested and centrifuged. The supernatant was discarded, and the cell pellet resuspended in 2 mL of medium. For growth inhibition assays, $0.75*10^5$ cells/mL were plated into flat bottomed 96-well plates (Costar, Corning, NY) and incubated at 37 ºC, 99 % humidity and 5 % CO_2 (v/v). Cell density was evaluated as the total number of viable cells within the grids on the hemacytometer (Hirschmann, Eberstadt, Germany) using trypan blue exclusion method. For this procedure 350 µL of medium was pipetted to a 2 mL eppendorf together with 50 µL of the 2mL cell suspension followed by 100 µL of 0.4 % (v/v) trypan blue solution (Sigma). The hemacytometer was loaded and examined immediately under the microscope at low resolution, and cell viability was determined through the equation 10.

$$\frac{\text{Nº of cells}}{\text{mL}} = \frac{\sum \text{cells per quadrant}}{4} * 10^4 \ (\text{Chamber Volume} * \text{Dilution factor}) \quad (10)$$

After 24 h, the samples were added (after removal of depleted medium), and the cells were incubated for an additional 48 h. Subsequently a reaction mix of medium, MTS (3-(4,5-dimethylthiazol-2-yl)-5-

(3-carboxymethoxyphenyl)-2-(4-sulfophenyl)-2H-tetrazolium, inner salt), and PMS (phenazine methosulfate) in a ratio of 100:19:1 was added to each well and further incubated for 45 min. During this period, MTS is bioreduced into formazan, by dehydrogenase enzymes present in metabolically active cells, which in turn is susceptible of being measured at 490 nm absorbance by Tecan Infinite F200 Microplate Reader (Tecan, Männedorf, Switzerland), directly from the 96-well assay plate, so that the quantity of formazan product measured is directly proportional to the number of living cells in culture. The cell viability results for each concentration assayed were normalized relative to the control samples and obtained accordingly to equation 11:

$$\frac{\text{Sample Absorvance (490 nm)}}{\text{Control Absorvance (490 nm)}} * 100 = \text{Cell Viability (\%)} \quad (11)$$

Before testing the powders, the drug was tested by itself at different concentrations (10, 50, 100 and 250 nM) and duration (24 and 48 hours). The assays were performed in duplicate.

2.3.13 Design of Experiment (DoE)

To understand the effect of some of the formulation variables on the particles size, a design of experiment (DoE) approach was adopted using STATISTICA™ software version 10 (Statsoft, Bell, Tulsa, Oklahoma). In this case the absence or presence of both L-leucine and BSA was tested, which means that 2^2 experiments were taken into account. All the experiments were made in triplicate and the statistical differences in between different formulations was obtained using Factorial ANOVA. The analysis was performed considering changes in Dv_{50}, MMAD, FPF and EF.

3. Results and Discussion

To study the production of microparticles for vaccine pulmonary delivery, while BSA was chosen as the model protein, since it has already been extensively studied and it also is safer to work with than an actual antigen; L-leucine was chosen as the bulking agent. While BSA and L-leucine are soluble in water, PLGA is not. The chosen organic solvent to dissolve PLGA was acetonitrile, since it was one of the few miscible in water and it also was the "greener" option. The quantity of water in the solution was diminished to a minimum, since CO_2 is partially soluble in it; therefore, the concentrations of BSA/L-Leucine used in the formulation were on their limit of solubility, as well as PLGA's.

Meanwhile, to treat pulmonary hypertension, neither the dendrimers nor the cholesterol, the chosen bulking agent, required the use of an aqueous solution, and ethanol and acetone were chosen to dissolve them respectively.

3.1 PLGA microparticles

Even though PLGA has been used as a carrier for pulmonary delivery in several research papers, there is no literature of it being micronized by SAA. Therefore, the first step of the process was to optimize the PLGA microparticles until the best operating conditions were found.

The temperature was a very important parameter to control due to the low T_g PLGA presents (45-50 ºC). When the mixture occurs in the static mixer, the temperature needs to be below this value, but yet, it has to be above the CO_2's critical temperature (31.1 ºC) and so 40 ºC was used as the set point, while the CO_2 was heated at 50 ºC. Other problem associated with the temperature was the efficient drying of the particles in the precipitator because the acetonitrile and water's boiling temperature (82 ºC and 100 ºC respectively) is much higher than the PLGA T_g. It was found that the best temperature to be used in the precipitator was around 70 ºC with compressed air entering at nearly 100 ºC. Temperatures below that led to wet particles, while temperatures much higher led to formation of melted particles. In order to maintain a heated flow until it reaches the cyclone, a heating tape was placed right after the precipitator.

As for the pressure, throughout the assays three different pressures were tested. At first a pressure of 10 MPa was used, and since the particles still required to be optimized, a higher pressure was tested but no differences were noticed. At last, a lower pressure was used (9 MPa) and there was a slight improvement in the particles characteristics, such as their size and morphology.

The gas to liquid ratio was calculated taking into account the volumetric flows and was varied between 5 and 1.55 but since there was a slight improvement with the higher ratio, the assays proceeded with it.

Other experimented option was the heating of the cyclone. This would ideally make sure that the solvent remained evaporated and the particles were dried. Instead it turned the particles more plasticized due to the polymer's T_g and to the fact that the particles were in contact with the heated surface throughout the entire assay.

Besides obtaining suitable particles' characteristics, another problem was the yield of the assays. They started out very low (5-10%), but with the optimization of the parameters they started to increase until they reached almost the 30%. Initially, two filters were used in the cyclone to improve the amount of powder collected, however because the PLGA particles are so small with sizes around the filter's pore diameter, they often obstructed the filter resulting in a fast pressure increase. The only way to perform an assay without the rise of pressure was to use a single filter inside the cyclone, which as a drawback, increased the amount of lost particles that left with the gaseous flow.

Table 3.1 shows some of the assays performed only with PLGA that showed major differences in yield and morphology.

Table 3.1- Operating parameters of some of the PLGA assays and the respective yields.

Assay	Yield (%)	T_{sat} (°C)	T_{prec} (°C)	$T_{pre-cyc}$ (°C)	T_{CO2} (°C)	T_{air} (°C)	Pressure (MPa)	Q_{CO2}/Q_{sol} Ratio[a]
1	10	n.a.	65	n.a.	180	180	10	5
2	23.6	45	n.a.	35	100	180	10	1.55
3	27.9	45	50	35	100	180	10	1.55
4	14.9	40	70	50	50	100	9	5

T_{sat} – Temperature of the saturator; T_{prec} – Temperature of the precipitator; $T_{pre-cyc}$ Temperature of the the pre-cyclone; T_{CO2} – Temperature of the carbon dioxide; T_{air} – Temperature of the compressed air; n.a. – not available. [a]Q_{CO2}/Q_{sol} ratio was obtained considering volumetric flows

3.1.1 Morphology

Although the first particles obtained were characterized for having geometric diameters much bigger than expected, their numeric diameters were smaller, and this can be explained by the existence of big agglomerates that even though were few in number, were large enough to make the geometric diameter increase to such high values, represented in Table 3.2. The first two assays showed agglomerates so large that only the 10x objective of Morphologi G3 was able to do the analysis, and which was probably not being capable of counting the smaller particles. When the most appropriate conditions were found, the agglomerates diminished from a diameter of around 200 μm to 10 μm.

To calculate the particles aerodynamic diameter the bulk density has to be taken into account. Because the particles have a small bulk density, when using the Stokes equation (1) to determine the d_a, the values decrease, even getting inside the appropriate range in the last assay.

Table 3.2 – Properties of PLGA microparticles

Assay	$D_{v,50}$ (μm)	$D_{n,50}$ (μm)	Span	Bulk Density (g/mL)	D_a (μm)
1	203.7(10x)	7.26	0.80		88.8
3	193.9(10x)	6.38	1.35	0.19±0.01	84.5
4	11.25±3.4	5.17±0.30	0.66±0.40		4.9

$D_{v,50}$= Particle volumetric diameter of 50% cumulative distribution; $D_{n,50}$ – Particle number diameter of 50% cumulative distribution;

Also to prove that the D_{v50} is due to the presence of agglomerates SEM was performed and the results are shown in Figure 3.1. As can be seen in the right side of the image (b) single particles do not have diameters much larger than 1μm. In the other hand, they do not seem spherical, but that is because when exposed to the electron beam of SEM, the particles tend to melt since they are heat-sensitive and lose their original form. Also by analyzing the images obtained by Morphologi G3 (Figure 3.2) it is possible to recognize the presence of agglomerates. The images (a;b) are from assay 3 particles and in (a) besides the expected particle aggregates there is also possible to see small single particles, while in (b) there is a confirmation that these big diameter particles are truly aggregates because their individual form is outlined. Comparing these to the images obtained in assay 4 the particle aggregates show a smaller size, and the presence of small particles is also confirmed.

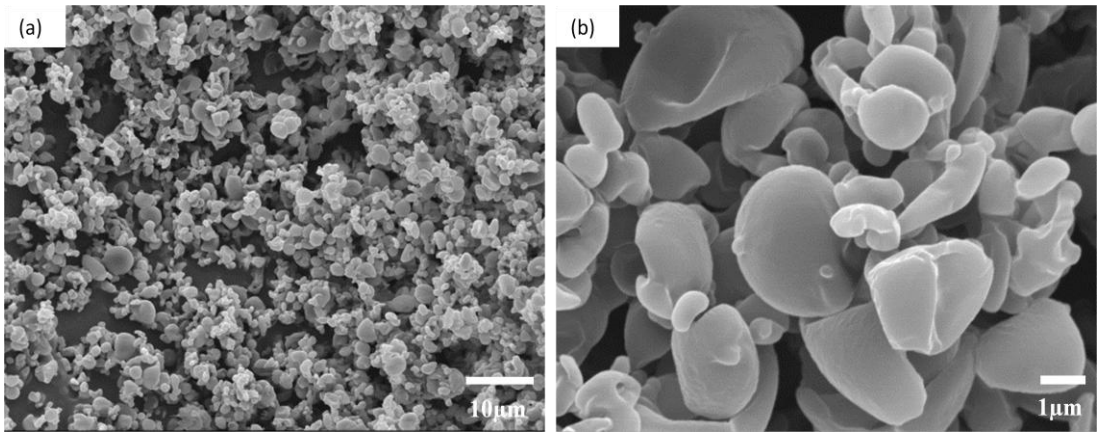

Figure 3.1 - SEM images of the PLGA microparticles with a magnification of (a) 1,500x and (b)10,000 x

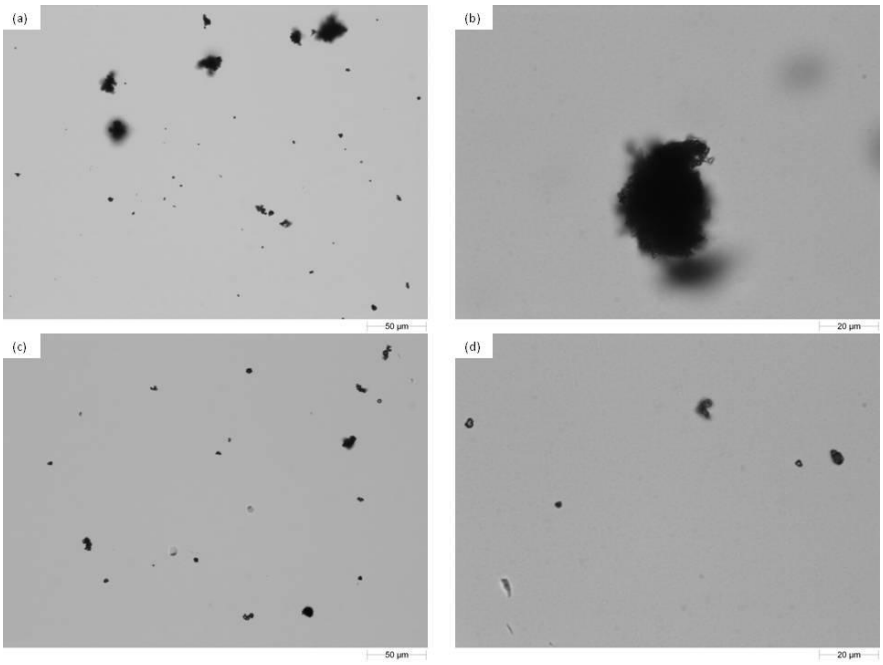

Figure 3.2 - Morphologi G3 images of the PLGA microparticles (a;b) at assay 3 and (c;d) 4. (a;c) and (b;d) used magnifications of 20,000 and 50,000 respectively.

3.1.2 Aerodynamic Performance

As already mentioned, the MMAD is also an important parameter when it comes to study particles suitable for inhalation purposes, and it is determined by the use of the ACI. The obtained result regarding the powders distribution is represented in Figure 3.3.

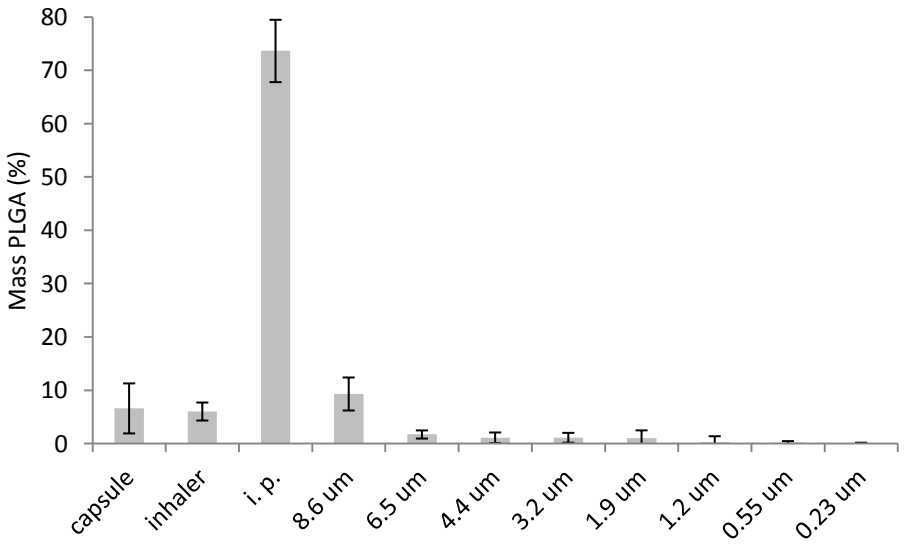

Figure 3.3- Graphical representation of the powder distribution in the ACI apparatus for the PLGA microparticles

By observing Figure 3.3 it is clear that most of the dry powder deposits in the induction port (IP), which is representing the upper airways, probably because of the aggregates presence and the formation of turbulent eddies in the curving zone of the tube, that has as a consequence the aggregates impaction. Besides the MMAD, there are other important values obtained through the ACI, such as the FPF and GSD. Recurring to the use of DUSA, the ED is also calculated and all these values are in Table 3.3 –. Taking into account that the MMAD of the formulation is around 7 μm, it was already expected that the FPF would be small, and this also explains the high quantity of powder deposited in the IP. The fact that the MMAD is so far from the d_a is probably due once again to the presence of the clogs that are not able to disaggregate when inhaled. Also the powder could not be uniform, leading to differences in sizes determined in different techniques. As for the ED, since it is above 98% it means that almost all the powder exits the capsule.

Table 3.3 – Representation of the aerodynamic properties determined by ACI and DUSA for the PLGA microparticles.

MMAD (μm)	FPF (%)	GSD	ED (%)
7.05±1.24	11.72±1.86	2.44±1.05	98.5±0.60

MMAD – Mass Median Aerodynamic Diameter; FPF- Fine particle fraction; GSD – Geometric Standard Deviation; ED – Emitted Dose

3.1.3 Physical-Chemical Properties

Given the importance of the solid-state of the particles, both unprocessed and processed by SAA PLGA was tested using XRD and the result is in Figure 3.4. They have very similar curves, both presenting a broad peak close to 20º showing that PLGA shows an amorphous state after and before being processed and thus making it suitable as a carrier.[84]

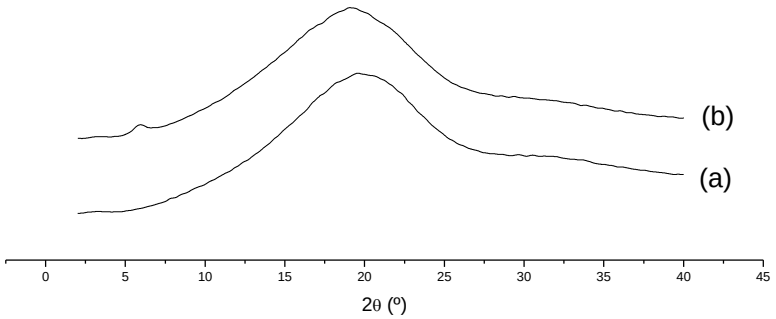

Figure 3.4 - X-ray Diffraction. (a) unprocessed PLGA; (b) PLGA microparticles

In Figure 3.5 are the DSC curves obtained for raw PLGA and PLGA microparticles and they both show a peak near the 50 ºC (46.2 ºC and 51.8 ºC respectively), which represents the polymer's T_g. Before and after this peak there is a slight step that represents a difference in the sample's Cp, and that corresponds to the glass transition of the polymer. The slight shift to the right might have been induced

by the micronization in SAA, since it is known that such process sometimes leads to increasing values of T_g.[81] There is a raise in the end of the curve at around 300ºC, which is attributed to thermal decomposition of the polymer.[85]

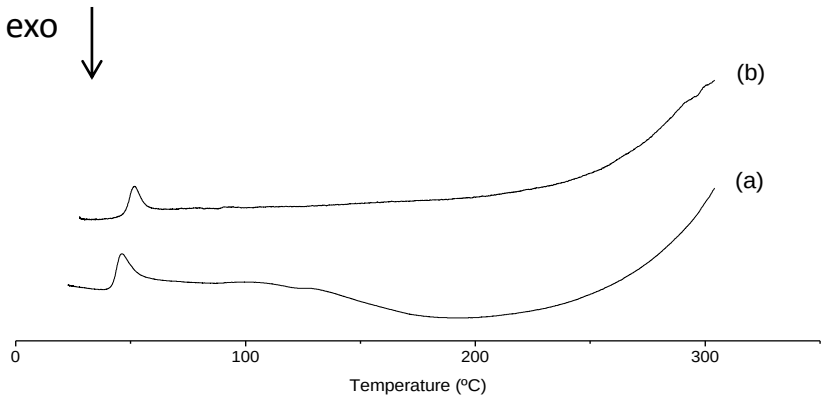

Figure 3.5 – DSC of (a) unprocessed PLGA and (b) PLGA microparticles

Both processed and unprocessed PLGA were analyzed by FTIR (Figure 3.6) in order to understand if the polymer was maintained in its conformation. Both spectra present the polymer's characteristic peaks: 3526/3528 cm^{-1} (OH strecthing), 2999 and 2955 cm^{-1} (C-H stretching of CH3 groups), 1760/1761 cm^{-1} (stretching of C=O) and 1088/1091 cm^{-1} (C-O strectching).[86,87]

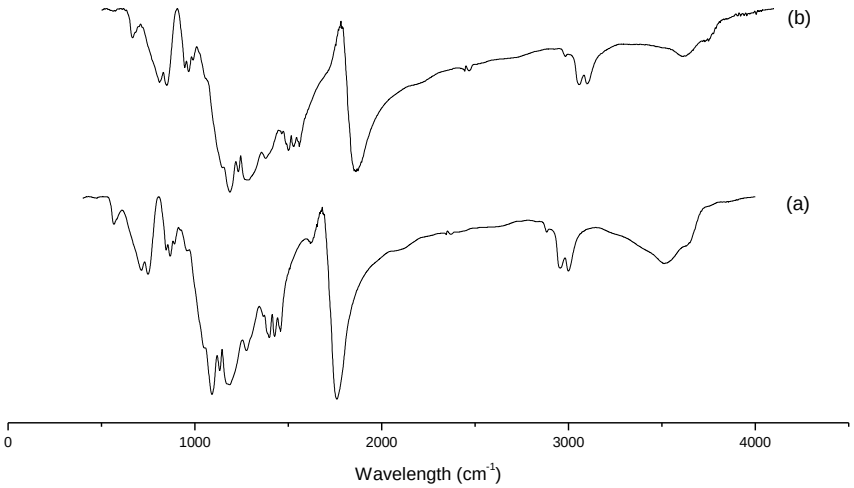

Figure 3.6 - FTIR. (a) unprocessed PLGA; (b) PLGA microparticles

In order to determine the water content of the particles, a Karl-Fischer test was performed and the resulting water percentage in PLGA particles is 0.86±0.07%, making clear that there is an efficient drying process.

3.1.4 Biodegradability Assays

The biodegradability of the PLGA particles was followed using solutions with and without lysozyme, an enzyme that is present in the lung, and the remaining weight as a function of time is in Figure 3.7. The biodegradation rate of the polymer is known to be around a month long, but in this experiment it took longer. When lysozyme is present the degradation is a bit faster, with a remaining weight of around 20%, while without lysozyme near 40% of the weight remained.
In spite of the results, a second experiment should be performed, since the original mass was very small, so slight differences in weight loss would be hard to notice, especially when the used scale was not the most appropriate because the changes within readings were in the apparatus error. Also, a longer time of lysozyme exposure should be considered, at least until the two months.

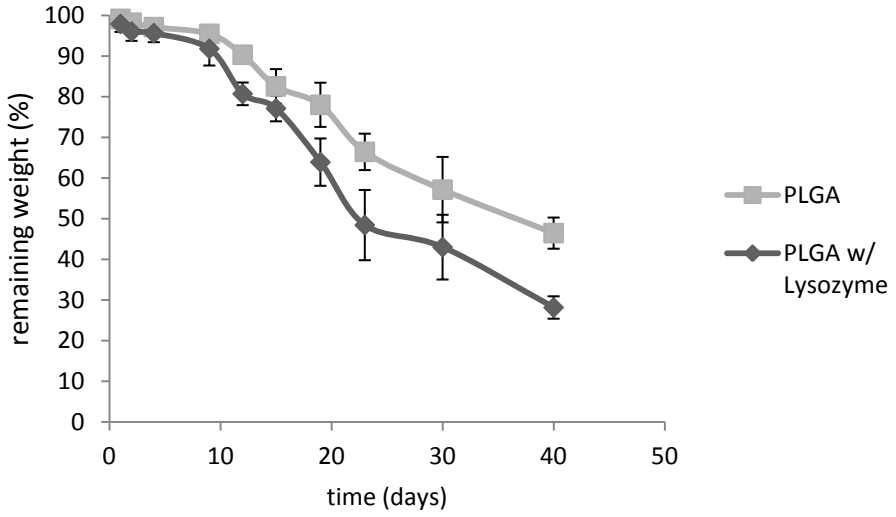

Figure 3.7 – Graphic representation of the PLGA degradation in a solution with and without lysozyme.

3.2 BSA-loaded microparticles

When the BSA was introduced in the microparticles, they showed a lot of improvements, yield and morphology-wise. Several conditions were tested for the new formulation and as expected the most suitable were the same ones used to produce PLGA microparticles. The ones that showed the biggest improvement are in Table 3.4 and the first point noticed is the increase in yield. When BSA was added, even though it is only 14% of the total mass, it was possible to see the improvements right away, because, besides the quantity, the presence of aggregates were not so evident and also the powder presented a better flowability. Since the solution was already at saturating conditions only other formulation with a different BSA concentration was tested (7% w/w), but as expected the resulting powder showed a decline in quality and quantity. The encapsulation efficiency of BSA in the

particles is about 48%. The low value of encapsulation can be due to BSA precipitation while it is being pumped until the static mixer.

Table 3.4 - Operating parameters of some of the BSA-loaded PLGA assays and the respective yields.

Assay	Yield (%)	T_{sat} (^oC)	T_{prec} (^oC)	$T_{pre-cyc}$ (^oC)	T_{CO2} (^oC)	T_{air} (^oC)	Pressure (MPa)	Q_{CO2}/Q_{sol} Ratio[a]
5	16	50	50	40	50	180	10	1.55
6	23.3	50	90	50	50	100	9	5
7	29.3	40	70	50	50	100	9	5

T_{sat} – Temperature of the saturator; T_{prec} – Temperature of the precipitator; $T_{pre-cyc}$ Temperature of the the pre-cyclone; T_{CO2} – Temperature of the carbon dioxide; T_{air} – Temperature of the compressed air. [a]Q_{CO2}/Q_{sol} ratio takes into account volumetric flows

In order to achieve better yields and improve the particles, L-leucine was added to the formulation, for the reasons already mentioned in the introduction, and tested at several concentrations being 14% w/w the highest possible amount of BSA and leucine combined. In assay 12 of Table 3.5 the particles were synthesized only with PLGA and leucine, and the yield went up to 30% so it was expected to see some gain in the yield by adding the three components together. After testing several ratios of leucine and BSA, at assay 11 the ideal mixture was found, with the highest acquired yield of 39%. The encapsulation efficiency was also calculated and for this formulation there is 59% of BSA encapsulation.

Table 3.5 - Operating parameters of some of the BSA-loaded PLGA assays using leucine and the respectively yield.

Assay	BSA/Leu ratio[a]	Yield (%)	T_{sat} (^oC)	T_{prec} (^oC)	$T_{pre-cyc}$ (^oC)	T_{CO2} (^oC)	T_{air} (^oC)	Pressure (MPa)	Q_{CO2}/Q_{sol} Ratio[b]
8	31	18.9	40	70	50	50	100	10	5
9	0.96	19	40	70	50	50	100	9	5
10	1.69	25	40	70	50	50	100	9	5
11	0.58	39	40	70	50	50	100	9	5
12	0	30	40	70	50	50	100	9	5

T_{sat} – Temperature of the saturator; T_{prec} – Temperature of the precipitator; $T_{pre-cyc}$ Temperature of the the pre-cyclone; T_{CO2} – Temperature of the carbon dioxide; T_{air} – Temperature of the compressed air. [a]BSA/Leu ratio takes into account the used mass. [b]Q_{CO2}/Q_{sol} ratio takes into account volumetric flows.

3.2.1 Morphology

By analyzing the diameters obtained in Table 3.6, there is an obvious difference in the D_{v50} of the particles with BSA, especially in the early assays. Once again by comparing the geometric and numeric diameters, there is a substantial difference justified by the same reason as before: existence of a few, yet large, agglomerates. The d_as, despite being in the suitable particle range, are in its very limit and since the improvement in size throughout the assays was not as big as expected, the use of a bulking agent was tested.

Table 3.6 – Properties of BSA-loaded PLGA microparticles

Assay	$D_{v,50}$ (µm)	$D_{n,50}$ (µm)	Span	Bulk Density (g/mL)	D_a (µm)
5	11.37±0.14	5.29±0.10	0.65±0.02		5
6	11.15±0.17	5.46±0.15	0.68±0.07	0.19±0.01	4.9
7	10.53±0.03	3.37±0.21	0.82±0.01		4.6

$D_{v,50}$= Particle volumetric diameter of 50% cumulative distribution; $D_{n,50}$ – Particle number diameter of 50% cumulative distribution;

Throughout the represented assays in Table 3.7 and by observation of the D_{n50}, it is possible to agree that the more leucine its added, smaller particles are formed. As for the D_{v50}, the assays with more leucine present more suitable diameters than when only BSA and PLGA were in the formulation. Also, these diameters are also smaller than the D_{v50} obtained for the particles containing PLGA and leucine, confirming that both BSA and leucine are important for the particles progress. This way, the d_as are better fitted into the needed range.

Table 3.7 - Properties of BSA-loaded PLGA microparticles using leucine.

Assay	$D_{v,50}$ (µm)	$D_{n,50}$ (µm)	Span	Bulk Density (g/mL)	D_a (µm)
8	11.07±0.03	3.80±0.22	1.83±0.57		4.82
9	10.79±2.39	4.46±0.54	0.74±0.63		4.70
10	7.38±1.10	2.82±0.45	1.54±0.05	0.19±0.01	3.22
11	9.39±0.98	2.48±0.54	0.98±0.14		4.09
12	10.75±0.80	2.63±0.12	0.80±0.13		4.69

$D_{v,50}$= Particle volumetric diameter of 50% cumulative distribution; $D_{n,50}$ – Particle number diameter of 50% cumulative distribution;

Besides differences in size, particles with encapsulated BSA also show differences in its morphology and in Figure 3.8 that difference can be noticed with the SEM images. The BSA-loaded PLGA microparticles (c;d) show a more spherical form and especially in (d) there are some particles with diameters smaller than 1µm. The analysis of the images obtained by Morphologi G3 (Figure 3.9) show the differences between particles. The images (c;d) are from BSA/leucine-loaded particles while (a) is from BSA-loaded particles and (b) is from leucine-loaded particles. By comparing the micrographs, it is clear the reduction in agglomerates from (a) to (d) and while the reduction from (b) to (d) is not certain, it is safe to say they both show fewer aggregates. In image (c) are magnified single particles that present a spherical form.

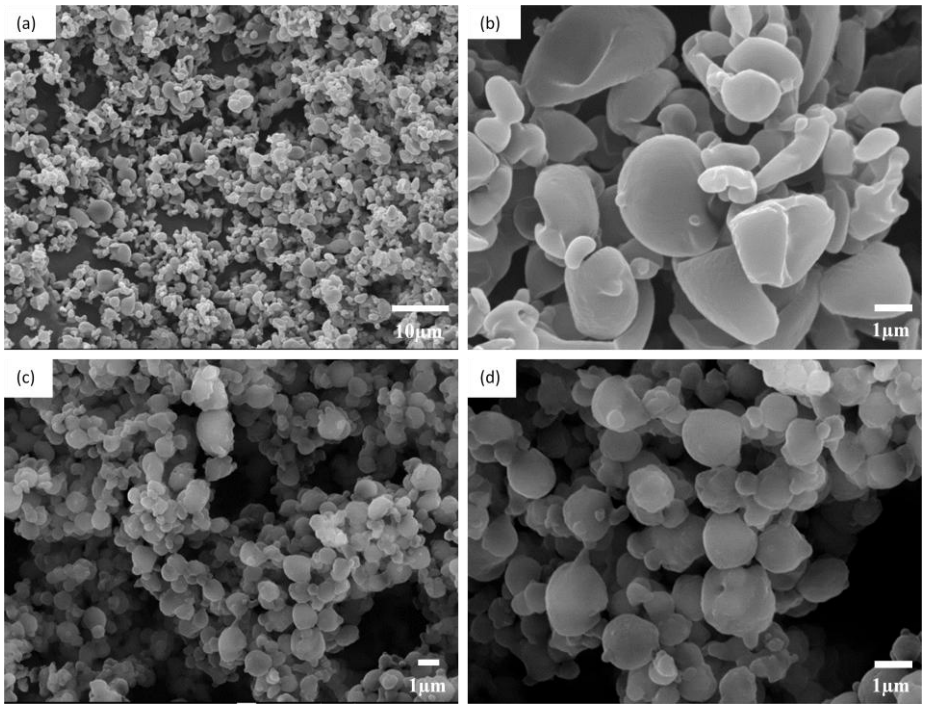

Figure 3.8 - SEM images of PLGA microparticles and the BSA-loaded PLGA microparticles with a magnification of (a) 1,500x (c) 5,000x and (b;d)10,000 x

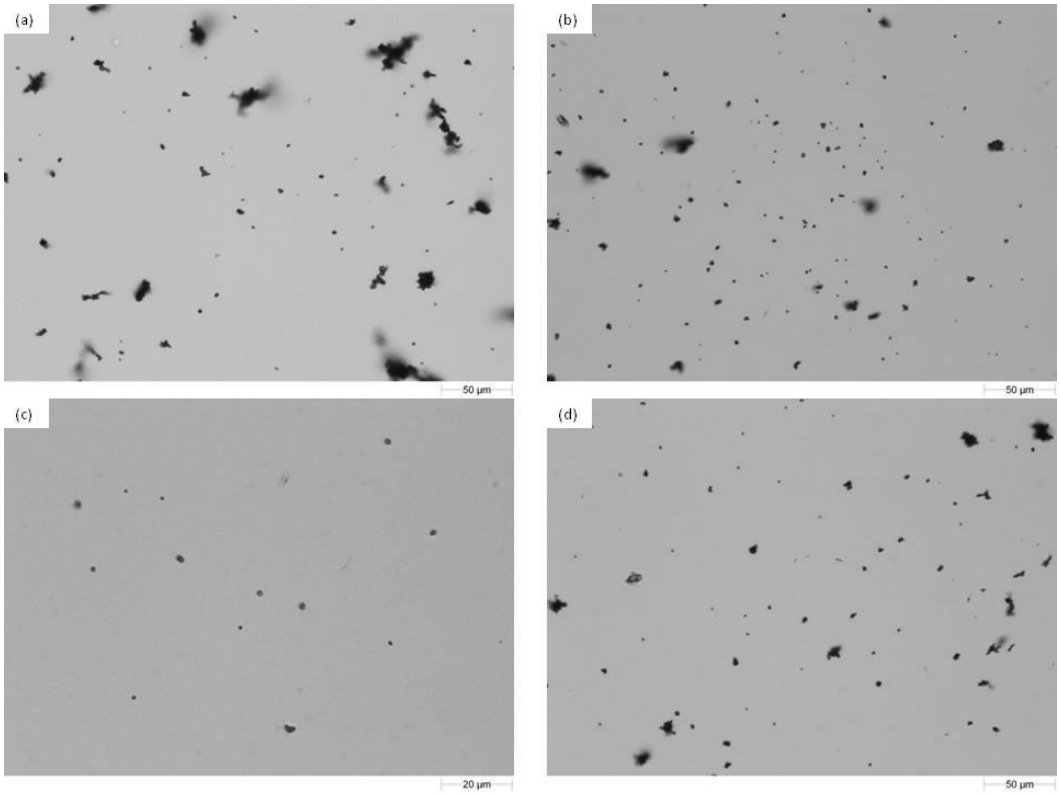

Figure 3.9 - Morphologi G3 images of the (a) BSA-loaded PLGA microparticles; (b) Leucine loaded PLGA microparticles; (c;d) BSA/leucine loaded PLGA microparticles. (a;b;d) and(c) used magnification of 20,000 and 50,000 respectively.

To understand the aggregates behavior when in contact with a solution replicating the one existing in the lung walls, a dispersion was performed into a droplet of a simulated lung fluid, containing the same components as the lung mucus. The solution was made taking into account a previously used one in the literature for the same use.[88] In Figure 3.10 is an example of an aggregate that when in contact with the solution for 10 min divides itself in smaller aggregates. However, there is no full disaggregation at least for the first 20 min.

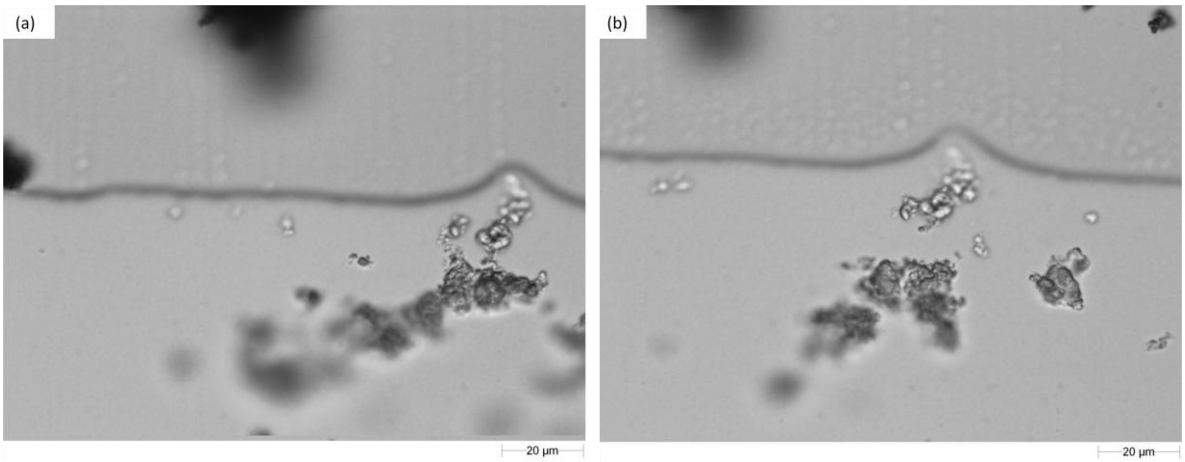

Figure 3.10 – Morphologi G3 images from BSA-loaded particles when in contact with a simulated lung fluid. (a) t=omin (b) t=10min. Images have a magnification of 50.000x

3.2.2 Aerodynamic Performance

The particles were then analyzed by ACI, and as expected, the results were better in comparison with the microparticles containing only PLGA. Both particles with and without leucine were tested, and the resulting distributions are represented in Figure 3.11. The main difference is in the decrease of powder deposited in the induction port, even though it is still a higher percentage than desired. Also, some of the further stages seem to have a slight raise. To confirm these, the MMAD and FPF were calculated and are in Table 3.8. Once again there is a slight difference between the MMAD and the d_a, probably meaning that there is some disaggregation while the particles are inhaled, leading to a smaller MMAD. There is an improvement in the FPF and GSD as well, especially when leucine is present, while the ED remains high. Although not very high, this value of FPF is within the range obtained for PLGA microparticles. [27,38]

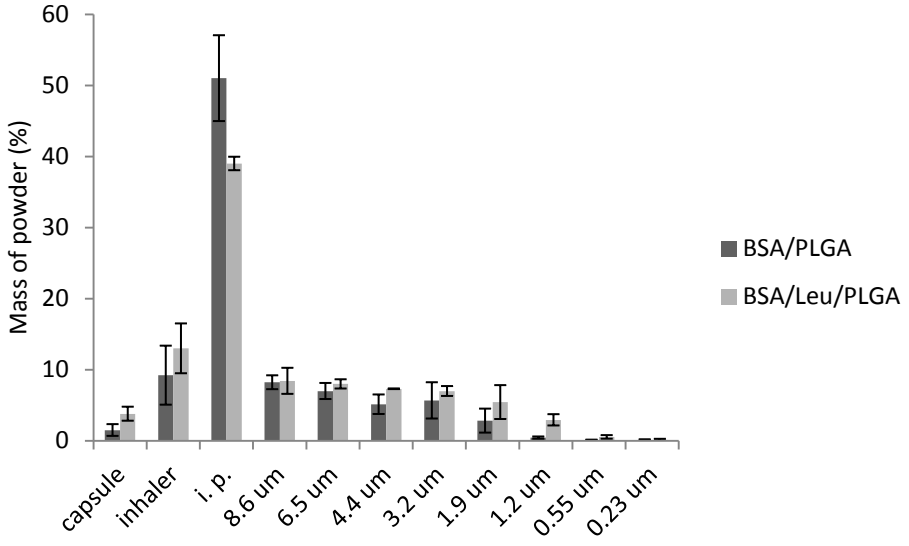

Figure 3.11 - Graphical representation of the powder distribution in the ACI apparatus for the BSA-loaded and BSA/Leu-loaded PLGA microparticles.

Table 3.8 - Representation of the aerodynamic properties determined by ACI and DUSA for the BSA-loaded PLGA microparticles.

	MMAD (μm)	**FPF (%)**	**GSD**	**ED (%)**
BSA	3.7±0.3	17±2	1.9±0.1	97.2±0.8
BSA/Leu	2.8±0.6	32±2	2.6±0.3	97.5±0.8

MMAD – Mass Median Aerodynamic Diameter; FPF- Fine particle fraction; GSD – Geometric Standard Deviation; ED – Emitted Dose

Even though it is possible to gather the mass of powder that gets to each ACI stage, the actual amount of BSA that is inhaled is not known. For that reason, the powder retained in each stage was dissolved and the BSA was quantified. Its distribution is in Figure 3.12 and it takes into account as total mass all the BSA that reaches every stage after de induction port, which in this case was 1.3±0.1 mg. This way the amount of BSA that reaches the deep lung can be estimated by quantification by UV.[70]

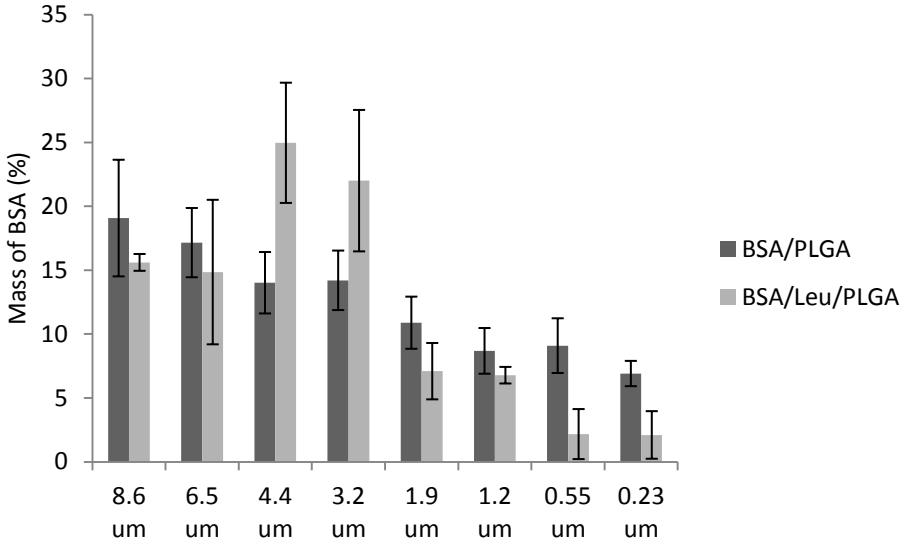

Figure 3.12 - Graphical representation of the BSA distribution in the ACI apparatus for the BSA-loaded and BSA/Leu-loaded PLGA microparticles.

When leucine is present the distribution of BSA throughout the stages was a bit different, being the stage with a cut-off of 4.41μm the one with the biggest quantity. Since the MMAD was decreased and the FPF increased, it is normal that more amounts of powder gets furthest, and by analyzing the Figure 3.11 this stage has a significant deposition. The distribution of BSA considers as a total mass 1.9±0.9 mg, which is also higher than without the presence of leucine.

3.2.3 Physical-Chemical Properties

The solid-state of all the produced particles was also studied. Both raw and processed BSA were represented in Figure 3.13, and the two curves have two peaks at about 7 and 20º, which indicates a presence of a semi-crystalline compound.[89]

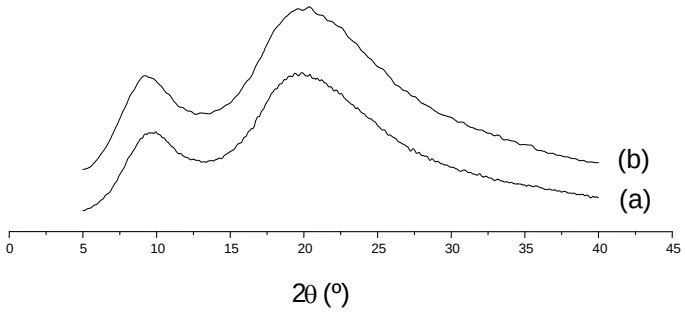

Figure 3.13 - X-Ray Diffraction. (a) unprocessed BSA; (b) BSA microparticles;

In Figure 3.14 the XRD curves of all the produced formulations are represented and it is possible to understand how the encapsulation of both leucine and BSA affect the particles solid-state.

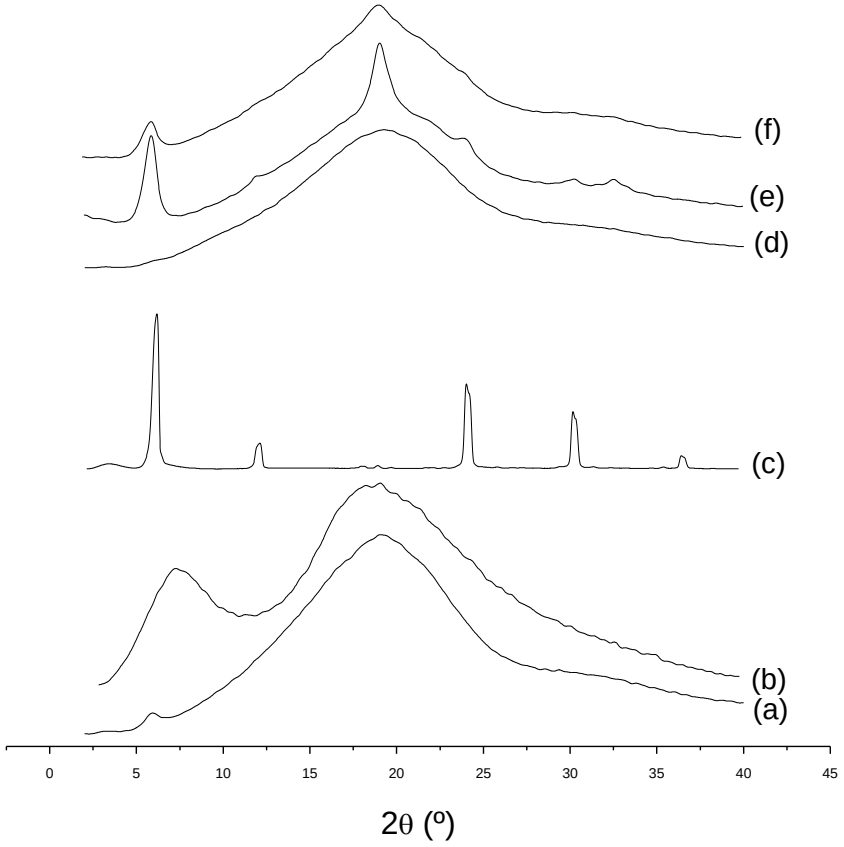

Figure 3.14 – X-Ray Diffraction. (a) PLGA microparticles; (b) BSA microparticles; (c)Leucine ; (d) PLGA-BSA microparticles; (e) PLGA-Leu microparticles ; (f) PLGA-BSA-Leu microparticles.

When BSA is encapsulated the peak is no longer noticed, which could indicate that all the BSA is within the polymer. When the leucine is added the curve gains two sharp peaks, which are proven to be from leucine by observation of curves. The curve (c) represents the XRD for raw leucine, which shows a crystalline form, and that is confirmed by the appearance of its peaks (6.12º, 24.39º and 30.61º).[90] However, when it is encapsulated in PLGA a new peak at about 20º appears which might indicate a structural change, while the peak at about 5º remains in the same position. When leucine is present in a small fraction, it tends to lose its crystalline form, which explains the fade of its peaks especially when BSA is encapsulated as well, because it has a very low concentration in this formulation.[91] Nonetheless, the fact that the peaks are still noticed indicates that leucine does not lose entirely its crystalline form.[91]

The DSC curves give complementary information of the XRD as can be seen in Figure 3.15. In all the DSC curves for PLGA, there is a peak near 50 ºC corresponding to the T_g of the polymer. Curve (b) presents a broad peak around 70 ºC, which is attributed to the melting point of raw BSA. Around this temperature, it is also expected to have a peak related to the reversible unfolding of protein chains. Also, there is a sharper peak at 225 ºC due to the full denaturation of the protein. However, by analyzing curve (c), this peak along with the broad one disappear suggesting the stability enhancement of the protein when entrapped in PLGA. Also, it might indicate the protein's dispersibility in the polymer's matrix.[91] The peak related to the polymer's T_g suffers a slight shift to the right (from 51.8 ºC to 53.7 ºC) which might be due to the overlap with the BSA's broad endothermic peak.[85,92] When leucine enters the formulation (d;e) a new peak appears at about 218 ºC that is correspondent to the leucine's decomposition.[93] Unlike BSA, this peak appears when leucine is micronized with PLGA and with both PLGA/BSA, which indicates the presence of a crystalline form, supporting the results obtained by XRD. The peak correspondent to PLGA suffers once again a shift (54.8 ºC in (d) and 55.5 ºC in (e)) indicating once again one possible interaction with leucine that leads to an increase in the T_g.

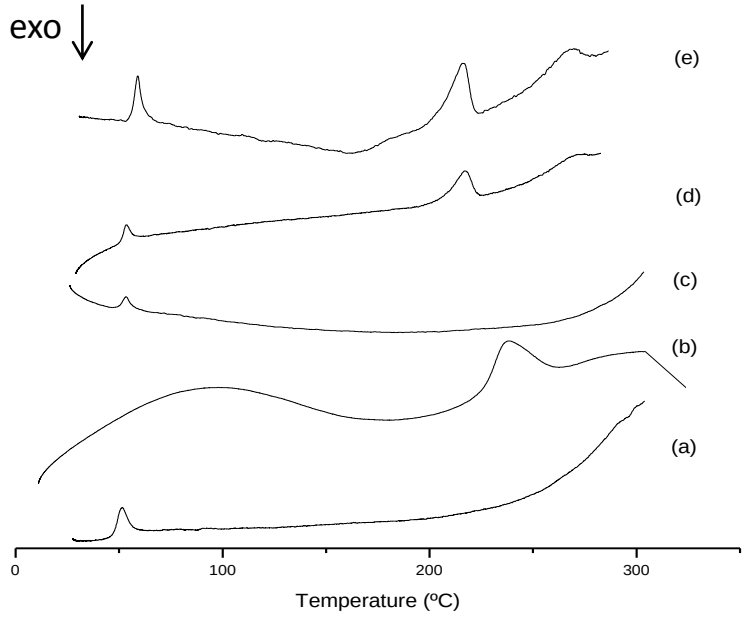

Figure 3.15 - DSC of (a) PLGA microparticles; (b) raw BSA; (c) BSA-loaded PLGA microparticles; (d) Leucine-loaded PLGA microparticles; (e) BSA/leu-loaded PLGA microparticles.

By the observation of the FTIR spectra in Figure 3.16 it is possible to notice that when the powder is constituted by PLGA and BSA there is an appearance of two peaks at 1655 and 1543 cm^{-1}, which correspond to the amide I (C=O stretching) and amide II (N–H bending) respectively. The PLGA peak correspondent to the OH suffered a shift from 3528 to 3302 cm^{-1}. The rest of the BSA peaks are masked by the polymer's peaks, which is understandable since the ratio of BSA and PLGA is near

1:10.[85]

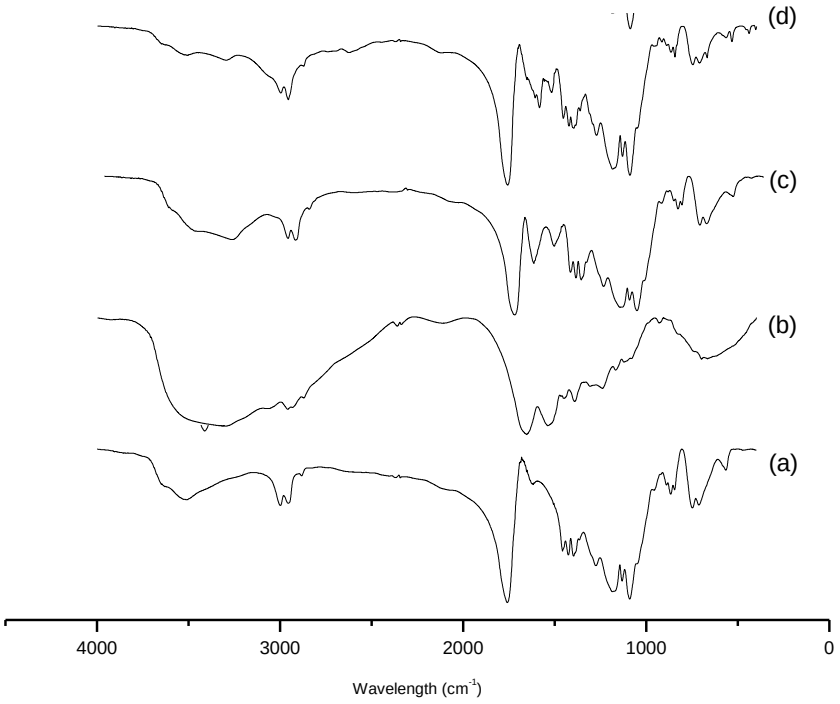

Figure 3.16 – FTIR. (a) PLGA microparticles; (b) BSA; (c) PLGA-BSA microparticles; (d) PLGA-BSA Leu microparticles

When leucine is added to the PLGA formulation the FTIR spectra (Figure 3.17) presents two new peaks observed at 1586 and 1522 cm^{-1}, which are associated to stretching vibrations of CO_2^-. These peaks suffered a minor shift to the left when compared to the leucine spectrum probably due to some conformational change. Also, the peaks at 3000 and 2955 cm^{-1} show a larger band which may happen by the influence of leucine's peaks at 2957 cm^{-1} which is due to asymmetric stretch of CH_2 group. The same happens when both BSA and leucine is added, and that can be confirmed by comparing it with the PLGA-BSA spectrum. Since both BSA and leucine present peaks between 1490 and 1650 cm^{-1} it is possible to see an increase of peaks in that area making it harder to identify them. As for the PLGA peak at 3528 cm^{-1}, it disappears when leucine is added, which might mean that there is some kind of bonding between the molecules.[94]

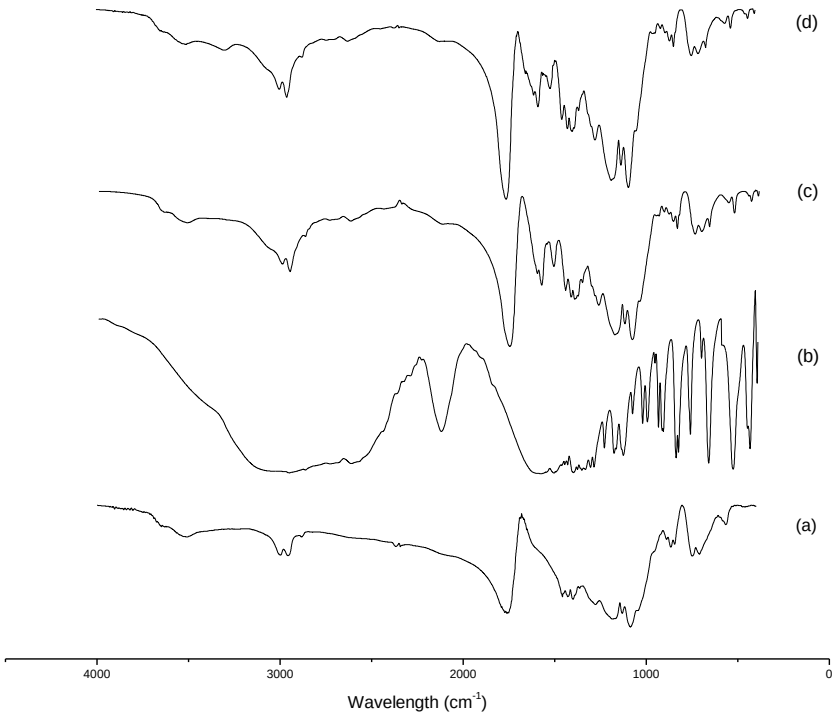

Figure 3.17 - FTIR. (a) PLGA microparticles; (b) Leucine; (c) Leu-loaded PLGA microparticles; (d) BSA/Leu-loaded microparticles

As for the particles' water content, the percentages of all the formulations are represented in Table 3.9 and in all of them it is safe to say that there is very few water in the particles, which reveals the drying efficacy of the SAA. Normally, the formulation with less water is the one that only contains PLGA, since this polymer is hydrophobic. Overall, when BSA and leucine are integrated in the formulation, the water content increases because these two compounds are hydrophilic. However, the particles with both leucine and BSA present the smallest percentage and this can be justified by the less formation of aggregates when in comparison with the other two formulations. Since the particles are looser they tend to dry more easily.

Table 3.9 – Water content values for the PLGA, BSA-loaded, Leucine-loaded and BSA/leucine-loaded PLGA microparticles

	PLGA	BSA/PLGA	Leu/PLGA	BSA/Leu/PLGA
Water content (%)	0.86±0.07	2.3±0.2	1.3±0.3	1.3±0.2

3.2.4 Pharmacokinetic Studies

By performing the pharmacokinetic studies it is possible to examine the BSA-loaded microparticles and to study the mechanism of its controlled release. The release curves were fitted using two different equations as represented in Figure 3.18 and Table 3.10. The Korsmeyer and Peppas equation (2) is only

suitable for 60% of the release and by the analysis of the n it can be concluded that when leucine is present the release is controlled by mostly Fickian diffusion (n=0.39) while when it is not present the swelling effect is the main cause for the BSA's release.[47] This might be explained by the interaction between leucine and PLGA that allows for an easier diffusion of BSA due to steric effects. Also, these particles have a slight decrease of agglomerates, meaning that the particles are looser and facilitate the BSA diffusion. Furthermore, in image (c) where the first two hours are represented, it is possible to see that the release when leucine is present is faster, releasing about 50% in a couple of hours while without it the 50% release is achieved at about 18hours. Meanwhile, with the use of the Peppas and Sahlin equation (3), which is already suitable for the 100% of release, both diffusion exponents lead to a Fick's diffusional release, as seen in image (b). Even though Fickian's diffusion is characterized for values of n<0.43, and the BSA release without leucine has a n=0.47, it is safe to admit that diffusion in the main present factor. Although both formulations have a different release rate, in both cases the 100% is achieved nearly 60hours within.

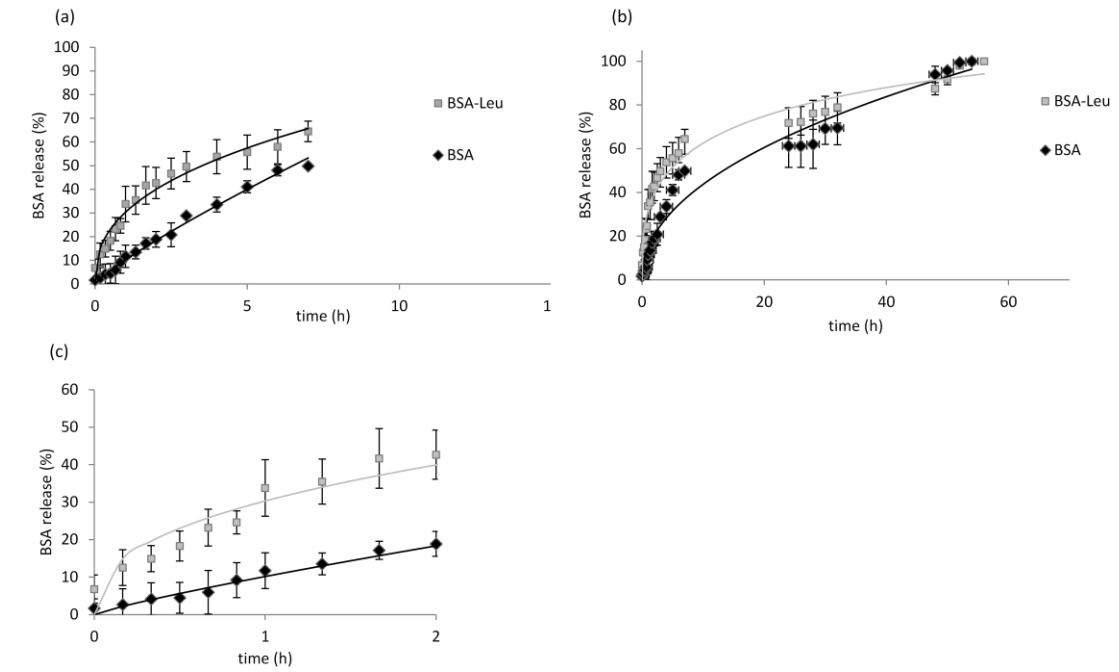

Figure 3.18 - Release profiles on the first 60% of BSA (a;c) and on the 100% release of BSA(b)adjusted with Kormsmeyer and Peppas equation and Peppas-Sahlin equation respectively. A zoom of the first two hours release is represented in (c).

Table 3.10 – Kinetic values obtained from the Korsmeyer Peppas and Peppas & Sahlin equations for the BSA-loaded and BSA/Leu-loaded PLGA microparticles-

Microparticles	Korsmeyer Peppas			Peppas & Sahlin			
	R^2	k	n	R^2	kd	kr	m
BSA/Leu	0.9467	0.0060	0.3969	0.9792	0.0165	-0.0017	0.3389
BSA	0.9907	0.0031	0.8500	0.9683	0.0212	-7E-6	0.4742

3.2.5 Biodegradability Assays

The degradation profiles of microparticles loaded with both BSA and leucine can be observed in Figure 3.19. The degradation rate is very similar to the PLGA microparticles, with a higher weight loss when lyzozyme is present and with a remaining 60% weight when not present. This slow degradation can be explained for the same reasons said before for the PLGA microparticles.

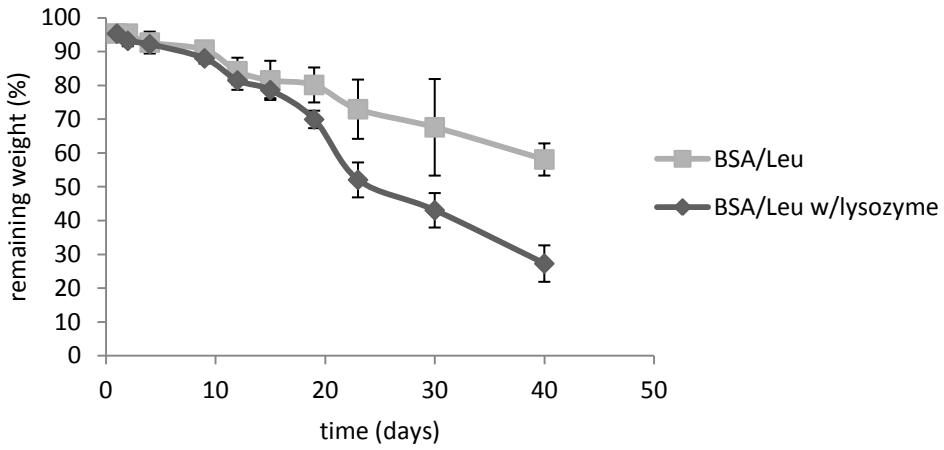

Figure 3.19 - Graphic representation of the BSA/Leu PLGA microparticles degradation in a solution with and without lyzozyme.

3.2.6 Biocompatibility

In order to confirm that the microparticles were not toxic to cells, a biocompatibility assay was performed using lung cells, the desired target. By the analysis of the results represented in Figure 3.20 it is clear that both BSA and PLGA are not toxic, once the percentages are all very close to the 100%, and that was already expected since they are known for their biocompatibility. Besides the produced microparticles show full cell viability, confirming that the SAA technique does not affect the components bioavailability.

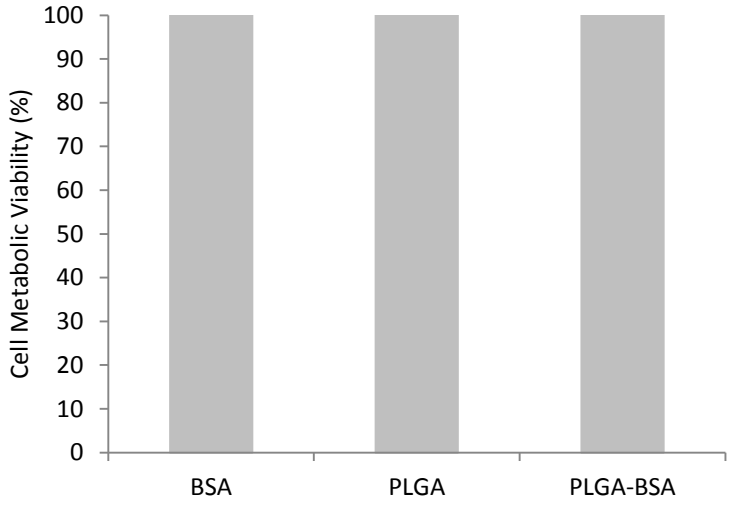

Figure 3.20 – Graphic representation of the BSA, PLGA and BSA/leu-loaded PLGA microparticles effect in cell viability.

3.2.7 Design of Experiment

In order to observe and actually confirm the effects of the addition of BSA and leucine, a design of experiment was performed and analyzed with the use of statistics. The variables that suffered a major difference were the MMAD, FPF and D_{v50} and these were the studied ones. With the analysis of the tables ahead it is possible to assume that for a significance value lower than 5%, MMAD is affected by the addition of BSA and leucine, as well as by the addition of both together (Table 3.11). The lowest *p*-value is obtained with the addition of BSA, being this factor the one that leads to the highest improvement of the MMAD. In Figure 3.21 is the effect of the addition of both BSA and leucine, and it is possible to see the big decrease of the MMAD when adding BSA and leucine, being the smallest MMAD the one with all the components.

Table 3.11 - ANOVA testing the effects of the parameters on MMAD for a significance level of 5%. *p*-values marked with * mean $p<0.05$; ** $p<0.01$; *** $p<0.001$; **** $p<0.0001$.

Effect	SS	Degree of freedom	MS	F	*p*-value
Intercept	256.69	1	256.69	461.57	0.0000
BSA	12.69	1	12.69	22.82	0.0014**
Leu	9.05	1	9.05	16.27	0.0038**
BSA/Leu	6.31	1	6.31	11.34	0.0098**
Error	4.45	8	0.56		

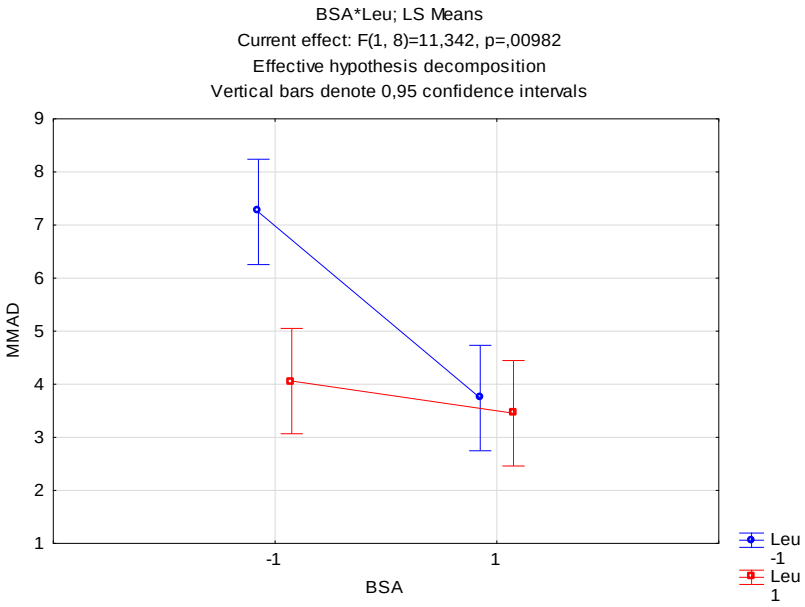

Figure 3.21 – Effect of BSA and leucine in the particles MMAD

When it comes to the FPF, taking into account the *p*-value in Table 3.12, the addition of BSA is the only factor that actually as an impact, which can also be seen in Figure 3.22 as the value increases in about 10 units.

Table 3.12 - ANOVA testing the effects of the parameters on FPF for a significance level of 5%. *p*-values marked with * mean $p<0.05$; ** $p<0.01$; *** $p<0.001$; **** $p<0.0001$.

Effect	SS	Degree of freedom	MS	F	*p*-value
Intercept	2236.14	1	2236.14	61.99	0.0000
BSA	269.14	1	269.14	7.46	0.0257*
Leu	27.09	1	27.09	0.75	0.4114
BSA/Leu	17.93	1	17.93	0.50	0.5007
Error	288.56	8	36.07		

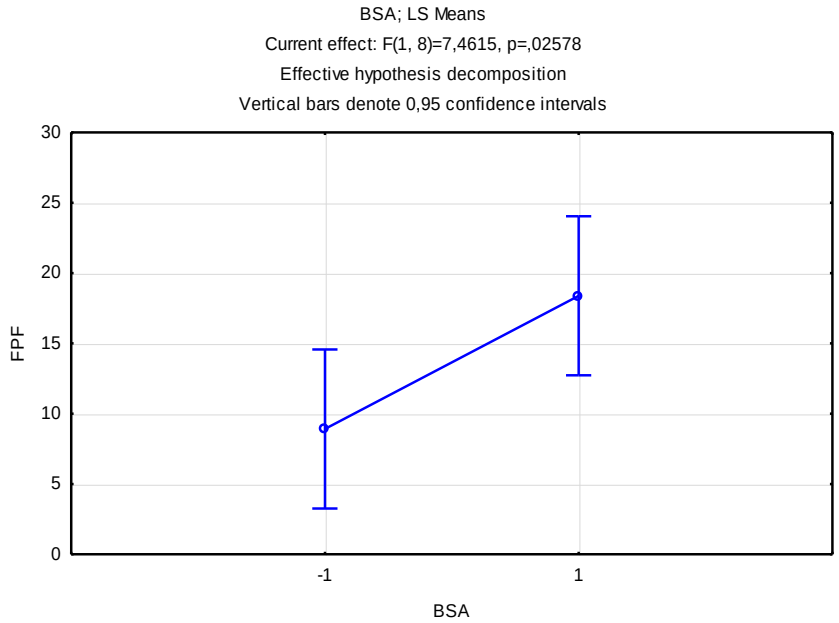

Figure 3.22 - Effect of BSA in the particles FPF

The D_{v50} is affected by the adittion of BSA and leucine, but leucine is the factor that most contributes to the decrease of the diameter as seen in Table 3.13. In Figure 3.23 is represented the effect of leucine and the difference is very high, with a decrease of nearly 8 μm in diameter. The ED was also evaluated, but since there were no major differences between assays there is no special effect on it from any of the additions, as confirmed in Table 3.14.

Table 3.13 - ANOVA testing the effects of the parameters on D_{v50} for a significance level of 5%. *p*-values marked with * mean $p<0.05$; ** $p<0.01$; *** $p<0.001$; **** $p<0.0001$.

Effect	SS	Degree of freedom	MS	F	*p*-value
Intercept	1376.45	1	1376.45	1887.55	0.0000
BSA	7.91	1	7.91	10.84	0.0109*
Leu	12.77	1	12.77	17.52	0.0030**
BSA/Leu	0.14	1	0.14	0.19	0.6766
Error	5.83	8	0.73		

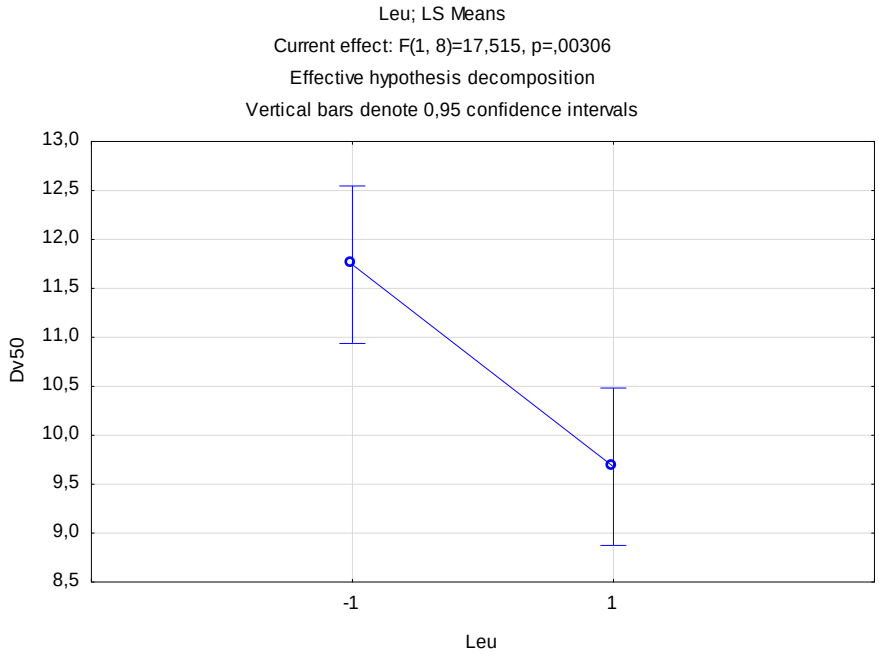

Figure 3.23 – Effect of leucine in the particles Dv50

Table 3.14 - ANOVA testing the effects of the parameters on ED for a significance level of 5%. *p*-values marked with * mean $p<0.05$; ** $p<0.01$; *** $p<0.001$; **** $p<0.0001$.

Effect	SS	Degree of freedom	MS	F	*p*-value
Intercept	115012.9	1	115012.9	68392.22	0.0000
BSA	0.1	1	0.1	0.03	0.8630
Leu	0.4	1	0.4	0.24	0.6374
BSA/Leu	5.1	1	5.1	3.01	0.1207
Error	13.5	8	1.7		

3.3 Dendrimer-loaded microparticles

When the formulation was based on the encapsulation of sildenafil-loaded dendrimers in PLGA microparticles at first, leucine was used as a bulking agent, and water, ethanol and acetonitrile were the chosen solvents. However, the particles did not show the desirable characteristics and the obtained yield was very low. For that reason, cholesterol was considered as the replacing bulking agent, which was advantageous, considering that it dissolved itself in acetone, permitting the exclusion of water from the solution. Since the amount of sildenafil-loaded dendrimers was not large, the first assays were performed only with PLGA and cholesterol. Then, the $PURE_{G4}$ dendrimers were added, and when the parameters were all set the sildenafil-loaded dendrimers were encapsulated. Two types of dendrimers were used, etil-oxazoline [$Pure_{G4}EtOx$] and metil-oxazoline [$Pure_{G4}MeOX$] dendrimers. With the use of both of them it is possible to understand the effect of their size in the particles

characteristics. As for the sildenafil encapsulation efficiencies, for the MEOx-SDF microparticles a percentage of 42.4% was obtained while the EtOx-SDF microparticles had an encapsulation percentage of 31.8% All the performed assays are in Table 3.15 as well as the characteristics used in each one of them.

Table 3.15 - Operating parameters of the dendrimers-loaded PLGA assays and the respective yields.

Assay	Yield (%)	T_{sat} (°C)	T_{prec} (°C)	$T_{pre-cyc}$ (°C)	T_{CO2} (°C)	T_{air} (°C)	Pressure (MPa)	Q_{CO2}/Q_{sol} Ratio[a]
PLGA/Chol	44.3	40	70	50	50	100	9	5
MeOx	51.0	40	70	50	50	100	9	5
EtOx	57.4	40	70	50	50	100	9	5
MeOx-SDF	58.3	40	70	50	50	100	9	5
EtOx-SDF	55.4	40	70	50	50	100	9	5

T_{sat} – Temperature of the saturator; T_{prec} – Temperature of the precipitator; $T_{pre-cyc}$ Temperature of the the pre-cyclone; T_{CO2} – Temperature of the carbon dioxide; T_{air} – Temperature of the compressed air. [a] Q_{CO2}/Q_{sol} ratio takes into account volumetric flows

The conditions were all very similar to the ones used with BSA microparticles, but as for the yields, those are quite better. The highest obtained yield was for the MeOx-SDF formulation at around 58% and it is in concordance with the other yields, since they tended to increase with the sildenafil encapsulation and also to be higher with [$Pure_{G4}$MeOx] than with [$Pure_{G4}$EtOx].

3.3.1 Morphology

By analyzing the diameters obtained in Table 3.16, it is possible to see that they are all around the 11 μm, being the smallest one with the [$Pure_{G4}$MeOx], which consequently presents the smallest aerodynamic diameter. When comparing the values obtained for the particles of PLGA/Chol with the ones with encapsulated dendrimers, it is possible to see that its addition led to reduced amount of aggregates. While PLGA/Chol has high numeric and volumetric diameters, caused probably by the existence of more aggregates, all the other formulations present a much smaller numeric diameter, confirming the presence of mostly small particles with only a few aggregates. When sildenafil is incorporated the resulting diameters remain in agreement given to the fact that both numeric and volumetric diameters of EtOx-SDF are higher than the MeOx-SDF.

Table 3.16 – Properties of dendrimer-loaded PLGA microparticles

Assay	$D_{v,50}$ (μm)	$D_{n,50}$ (μm)	Span	Bulk Density (g/mL)	D_a (μm)
PLGA/Chol	11.87±0.47	7.04±0.02	0.71±0.04		5.17
MeOx	9.02±0.27	2.49±0.49	1.3±0.3		3.93
EtOx	10.27±1.55	3.95±0.44	0.67±0.02	0.19±0.01	4.47
MeOx-SDF	9.84±0.20	2.47±1.50	0.7±0.4		4.28
EtOx-SDF	10.59±0.14	2.88±0.32	0.64±0.06		4.62

$D_{v,50}$= Particle volumetric diameter of 50% cumulative distribution; $D_{n,50}$ – Particle number diameter of 50% cumulative distribution; Span= $(D_{90}-D_{10})/D_{50}$

The particles containing the dendrimers were even more sensitive to the electron beam of the SEM analyzes and so the images obtained show a lot of melted particles, which lost their form and so it became impossible to check on their size or shape. On the other hand, it was possible to obtain the Morphologi G3 results as seen in Figure 3.24. There is no noticeable difference between the images, because all the diameters are so close to each other. All show single-small particles as well as some aggregates with sizes around 20µm.

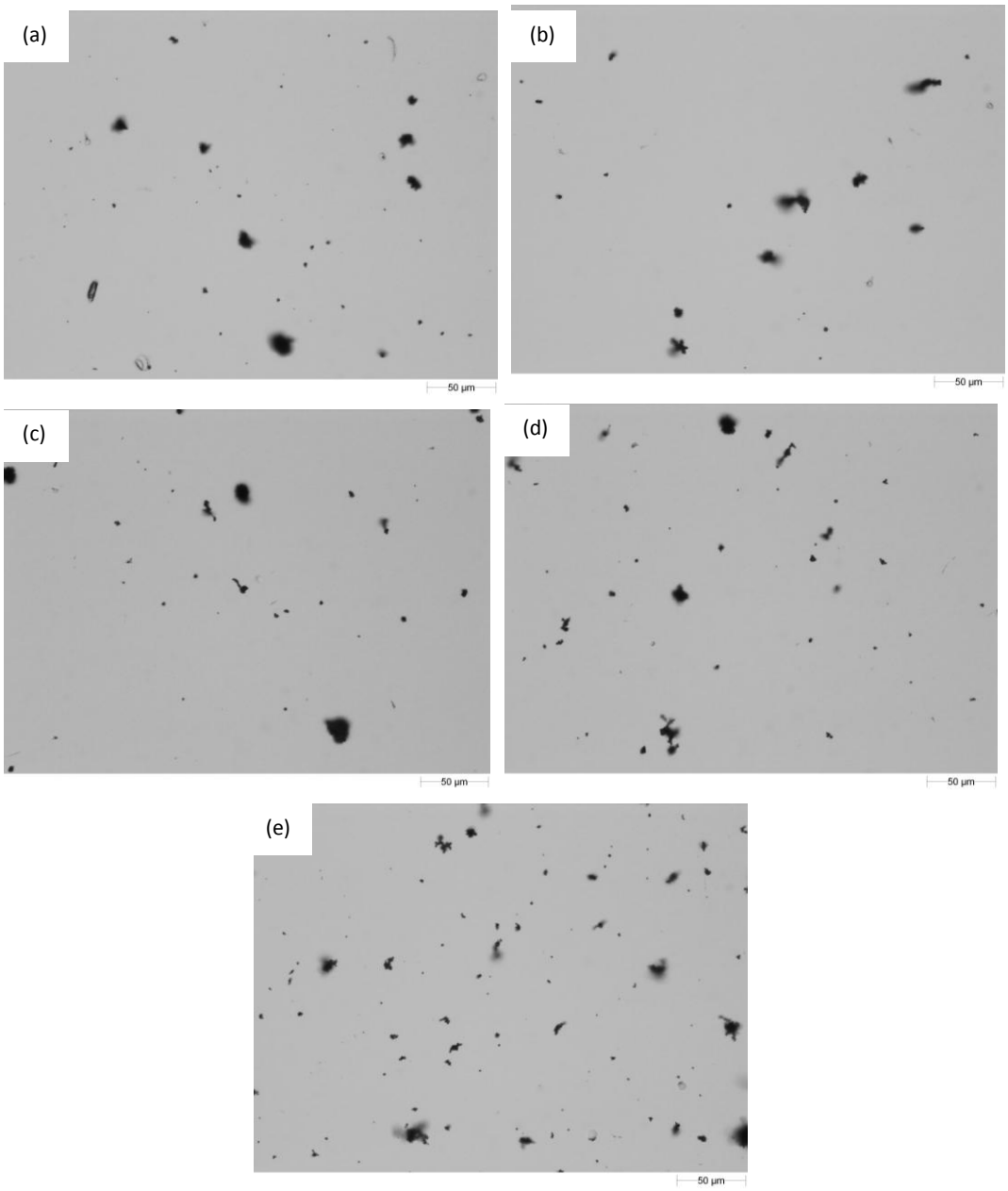

Figure 3.24 - Morphologi G3 images of the (a) Meox; (b) EtOx (c) MeOx-SDF; (d) EtOx-SDF; (e) PLGA/Chol. The used magnification was 50,000x.

3.3.2 Aerodynamic Performance

The particles were then analyzed by ACI, and the results of the several formulations are presented in Figure 3.25. The particles containing the drug were not tested for a matter of security and also because the drug is in such a low percentage that its presence was not expected to change the results. They all present similar distributions, being the main problem the high particle deposition in the induction port. All the formulations present about 50% or less of particle deposition in the area, being the highest value the one for PLGA/Chol particles, which was already expected considering the calculated diameters. Both dendrimers show a similar percentage deposition in all the stages of the ACI, and also the associated error for the MeOx particles is high, indicating the lack of particles uniformity.

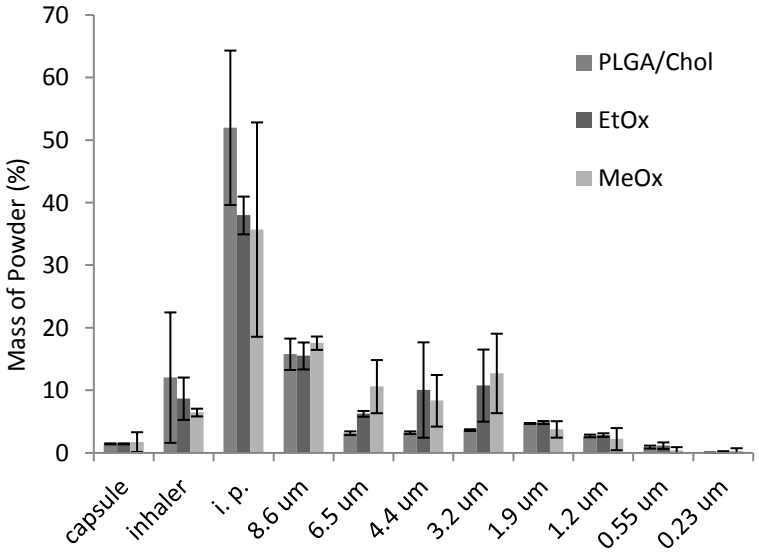

Figure 3.25 - Graphical representation of the powder distribution in the ACI apparatus for the cholesterol-loaded and dendrimer-loaded PLGA microparticles.

Analyzing Table 3.8, it is possible to see that the formulation containing dendrimers present a more suitable MMAD and FPF, showing that their presence improves the aerodynamic properties of the particles. The MeOx formulation presents the best MMAD and FPF, which is in concordance with the calculated diameters and as for the distribution throughout the ACI states it is hard to establish a connection due to the associated errors.

Table 3.17 - Representation of the aerodynamic properties determined by ACI and DUSA for the cholesterol-loaded and dendrimer-loaded PLGA microparticles.

	MMAD (μm)	**FPF (%)**	**GSD**	**ED (%)**
PLGA/Chol	4.55±0.09	16.37±0.09	2.0±0.4	98.7±0.6
EtOx	3.0±0.7	29±2	2.3±0.3	98.4±0.2
MeOx	2.57±0.09	36±4	2.41±0.05	94.4±0.8

MMAD – Mass Median Aerodynamic Diameter; FPF- Fine particle fraction; GSD – Geometric Standard Deviation; ED – Emitted Dose

3.3.3 Physical-Chemical Properties

The solid-state results are in Figure 3.26 and are much different that the ones obtained with the other particles. In image (a), where it is represented the PLGA/Chol particles, the curve presents several peaks, but since they are not very sharp and also a broad peak is noticed, it is possible to say that the compound is semi-crystalline. It is shown that this type of particles exhibited lower specific surface energy leading to a better performance in the powder flow and aerosol tests than crystalline materials.[95] That remains visible throughout all the particles, and because there is no XRD information on the dendrimers it is possible to admit that their encapsulation does not change the particles solid-state characteristics.

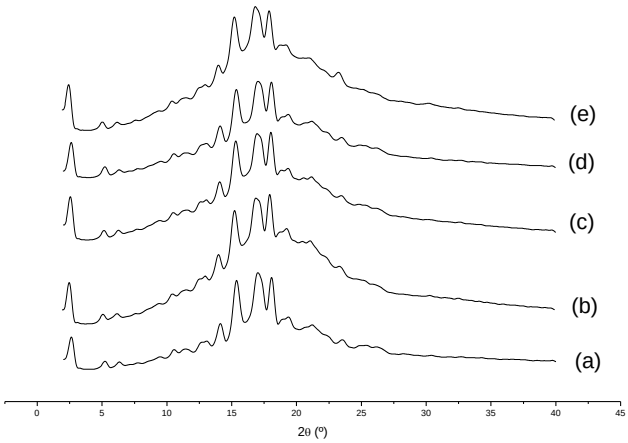

Figure 3.26 – X-ray Diffraction. (a) PLGA-Chol; (b) MeOX; (c)EtOx; (d) MeOX-SDF; (e) EtOx-SDF

The DSC curves represented in Figure 3.27 all have in common a small peak at about 50 ºC which is from the T_g of PLGA. A new sharp peak at 150 ºC appeared, due to the presence of cholesterol.[96] When the dendrimers are part of the formulation the cholesterol peak tends to fluctuate within a small range, while it also suffers some broadening, indicating its distribution in the polymers mixture.

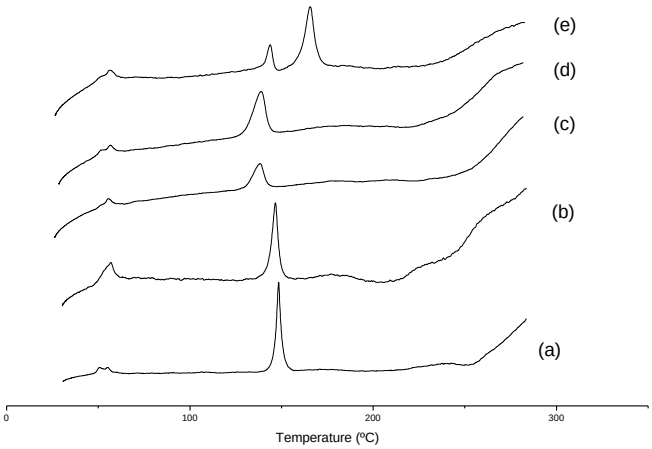

Figure 3.27 – DSC. (a) PLGA-Chol; (b) MeOx; (c) EtOx; (c)MeOX-SDF; (e)EtOx-SDF.

Also, the FTIR spectra obtained are in Figure 3.28. When comparing the FTIR spectra of the dendrimer-loaded particles with the PLGA/Chol particles, a peak appearance is seen at 1636 cm^{-1} (1627 cm^{-1} in MeOx-SDF), which corresponds to the C=O from urea. Also there is an increase of the band at 3420 cm, (3433 cm in MeOx-SDF) which corresponds to the amino groups of the dendrimers. As already noticed the MeOx-SDF shows a slight shift to the left and as for the MeOx, the dendrimer characteristic peaks are barely noticed which can be explained by a smaller concentration of it in the particles. In the spectra containing sildenafil there is no diference but that was expected since the quantity of drug is very small when in comparison with the dendrimer and excipients.

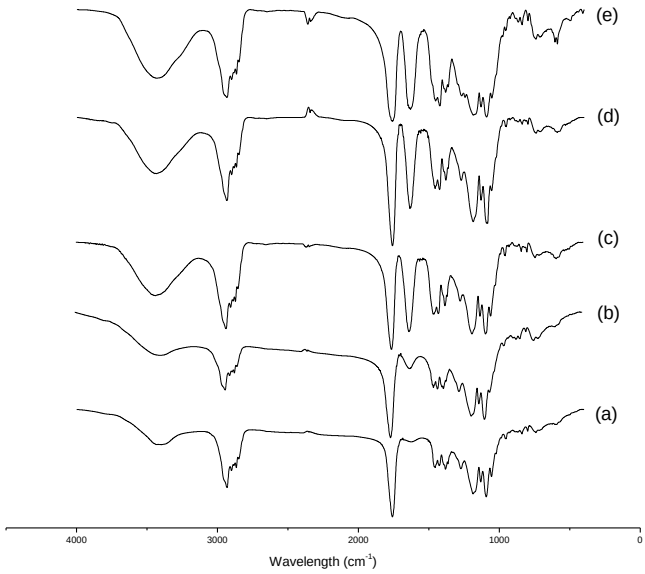

Figure 3.28 – FTIR. (a) PLGA-Chol; (b) MeOX; (c) EtOx; (d) MeOX-SDF; (e) EtOx-SDF

As for the particles' water content, the percentages of all the formulations are represented in Table 3.18. The particles containing only PLGA and cholesterol show the smallest amount of water, what was already expected since, they are both hydrophobic and especially because this formulation does not use water as a solvent, and that explains the value under the one obtained for PLGA particles. However, dendrimers are very hygroscopic and thus tend to gain humidity with time, which was probably what happened and why the water content increased relatively to the PLGA/Chol. Despite that, all the values remain very low, and it is clear that they all present a very dry state.

Table 3.18 - Water content values for the PLGA, BSA-loaded, Leucine-loaded and BSA/leucine-loaded PLGA microparticles

	PLGA/Chol	MeOx	EtOx
Water content (%)	0.49±0.04	2.37±0.06	1.98±0.07

3.3.4 Pharmacokinetic Studies

In order to study the release of the SDF from the micoparticles, the pharmacokinetic studies were performed. The Korsmeyer and Peppas equation (2) is represented in Figure 3.29 while the kinetic values obtained from it are in Table 3.19 and by the analysis of the n it can be concluded that either with MeOx and EtOx the release is controlled by mostly Fickian diffusion. Also, in images (c;d) where the first few hours are represented, it is possible to see that the release whit a pH of 5.5 is faster, releasing about 50% in less than an hour while with a pH of 7.4 the 50% release is achieved at about 2 hours. That can be justified by the polymer's faster degradation at acidic pH, since this condition tends to catalyze the breakage of the ester linkage of PLGA, leading to its erosion.[97] With this it becomes

much easier for the dendrimers to release themselves in the solution by diffusion and consequently release the sildenafil.

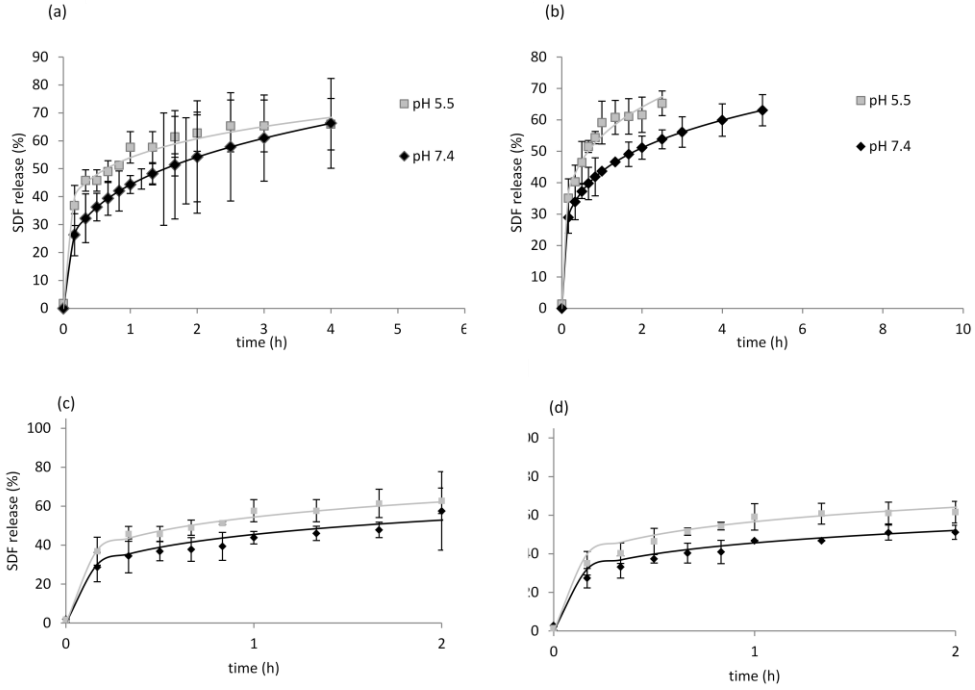

Figure 3.29 - Release profiles on the first 60% of Sildenafil of (a;c) EtOx-SDF and of (b;d) MeOx-SDF adjusted with Kormsmeyer and Peppas equation.

Likewise, with the use of the Peppas and Sahlin equation (3) as showed in Figure 3.30 and Table 3.19, the curves are all defined by a Fickian diffusional release. In this formulation the release is much faster in the beginning but it eventually slows down since the 100% release is achieved at nearly 80 hours within.

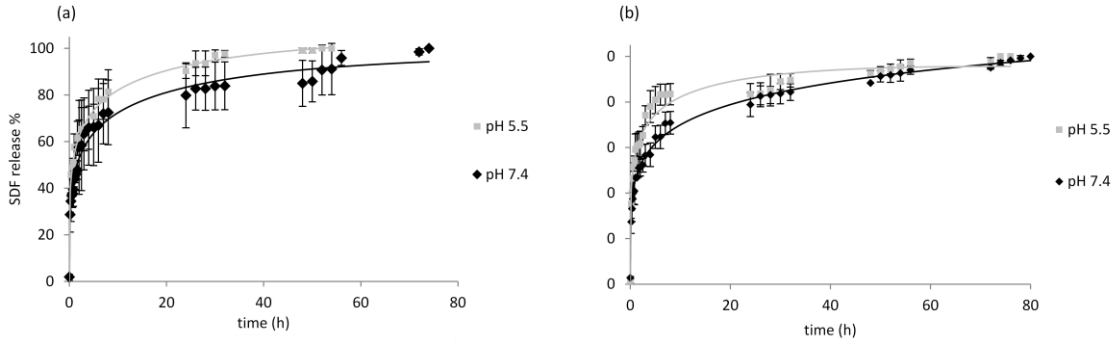

Figure 3.30 - Release profiles of Sildenafil of (a) EtOx-SDF and of (b) MeOx-SDF adjusted with Peppas and Sahlin equation.

Table 3.19 – Kinetic values obtained from the Korsmeyer Peppas and Peppas & Sahlin equations for the dendrimer-loaded PLGA microparticles.

Microparticles	pH	Korsmeyer Peppas			Peppas & Sahlin			
		R^2	k	n	R^2	kd	kr	m
EtOx	5.5	0.9980	0.2680	0.1707	0.9957	0.1790	-0.0008	0.2636
	7.4	0.9899	0.1350	0.2902	0.9808	0.2380	-0.0137	0.2430
MeOx	5.5	0.9983	0.2200	0.2233	0.9679	0.2080	-0.0008	0.2159
	7.4	0.9988	0.1710	0.2289	0.9944	0.2380	-0.0137	0.2430

3.3.5 Biodegradability Assays

The several formulations were tested for the biodegradability when in contact with lysozyme, an enzyme present in the lungs. The remaining weight throughout time is represented in Figure 3.31 and it shows information regarding the PLGA microparticles as well as the particles with encapsulated dendrimers. After the first 20 hours, there is a slower release, stabilizing at the 40 days. PLGA particles show less release than in the other formulations, ending up with a higher mass percentage than the others.

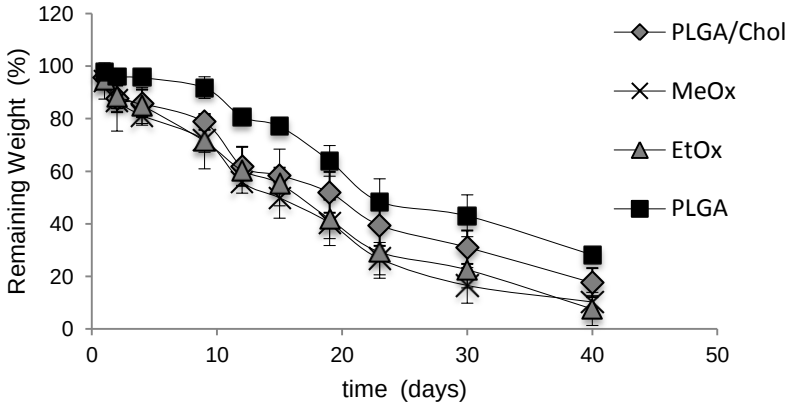

Figure 3.31 – Graphic representation of the biodegradation of PLGA microparticles, PLGA/Chol, MeOx and EtOx microparticles

3.3.6 Biocompatibility

Before studying the availability of the microparticles, the possible toxicity of the sildenafil at several concentrations and activity times was tested. As seen in Figure 3.32 concentrations between 10 nM and 100 nM do not present any toxicity to lung cells. However, at concentrations of 250 nM the viability percentage presents some decrease, going around the 80% at (a) and 70% at (b). For that, and to see the effect of the sildenafil encapsulation, the assays were carried on using sildenafil at a concentration of 250 nM and an activity of 48hours.

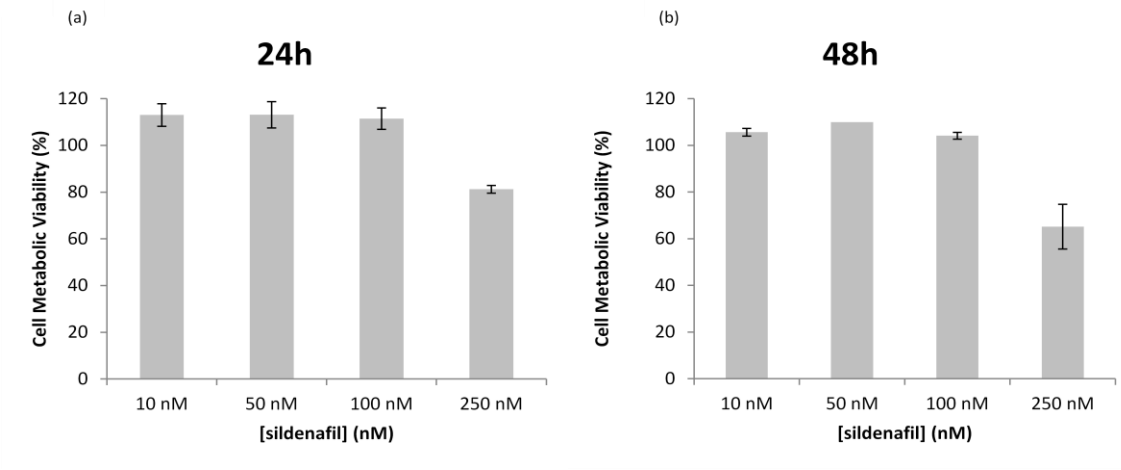

Figure 3.32 - Graphic representation of the 24hour (a) and 48 hour (b) sildenafil effect in cell viability.

The viability of the dendrimers-loaded microparticles was also tested to work as a blank. By the analysis of the Figure 3.33 is possible to see that the viability stands near 100% in all the cases, with the exception of EtOx-SDF, whose value is near the 140%. Since it is an isolated case, it could just be due to higher cell content in the well, associated with a cell seeding error. Also, the viability obtained for sildenafil-encapsulated particles in Figure 3.33 is higher than the one obtained for free sildenafil in Figure 3.32, which shows how the encapsulation process diminishes the toxicity of the compound, possibility due to the controlled release of it. Overall, it is safe to say that all the particles show full viability and are not toxic to lung cells.

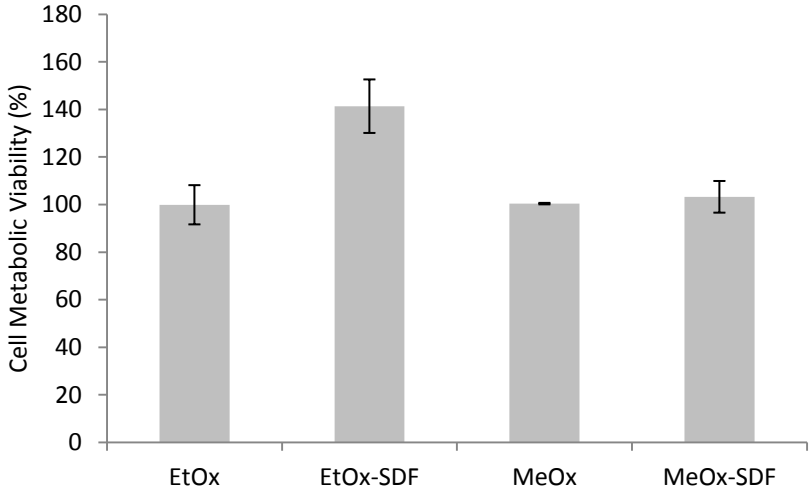

Figure 3.33 - Graphic representation of the dendrimer-loaded PLGA microparticles; SDF-dendrimer-loaded PLGA microparticles and of sildenafil effect in cell viability.

4. Discussion

When taking into account the overall results obtained there are some major aspects that can be noticed. In general, the particles showed mean volumetric diameters of about 11 μm, with correspondent number distribution diameters between 3 and 7 μm, which showed the existence of large aggregates in the powder. With the results obtained by Morphologi and SEM this aspect was confirmed. Even though it shows some variance, the present agglomerates affected all the formulations, indicating a problem associated with the manufacturing technique. Because PLGA is a polymer with a very low glass transition temperature it becomes an obstacle to produce particles with a technique that requires reasonably high temperatures. The parameters chosen to proceed with the production were the ones that led to the most suitable particles in terms of size, morphology and aerodynamic properties, all crucial characteristics to take into account when producing inhalation dry powders, but one must bear in mind that these parameters are still affecting the production. Even though the final product presents an aspect of a dry powder, it is possible that some melting is happening, making the particles attach to each other.

However, these microparticles present a low density (0.19±0.01 g/mL), which is a major advantage for its aerodynamic performance, caused by the CO_2 expansion and consequent droplet burst, and affected directly the obtained aerodynamic diameters (4.9 μm for PLGA microparticles; 3.22 μm for BSA/leu and 3.93 μm for dendrimer/chol formulations). As was already mentioned before, ideally particles should have a high diameter associated with a low density, in a way that the macrophages would avoid them and still they would have the flowability that would allow them to reach the deep lung. [98]

With the results obtained with the ACI, this property is also visible, with values of MMAD between 2 and 7 μm. Even though some of these values are still higher than desired, some of the powders fit in the proper range and are suitable for inhalation[36], and those correspond to the PLGA microparticles with both API and bulking agent. There is a very accentuated difference between the MMAD and FPF values obtained for the PLGA microparticles (7.05μm and 11.72% respectively) and than the ones with encapsulated BSA/Leu (2.82 μm and 31.73%) and dendrimer/Chol (2.57 μm and 36.46%), showing that for both cases the addition of these compounds was in fact crucial. A major concern that is visible when performing the aerodynamic tests is the amount of powder that deposits in the induction port. Even though this is usual, as already mentioned, the percentage range is under the one observed with already obtained inhalation PLGA particles.[99] It is also known that this deposition is highly related mainly to the presence of the aggregates[100,101] and as a consequence the values of FPF obtained were low, with a maximum of 36%. It is known that DPIs of the first generation commonly exhibited a relatively low efficiency in terms of the FPF. The efficiency of the microparticles entrainment resides on the ability of the DPI to generate forces sufficient to deagglomerate the powder and create a high flow, and that becomes hampered when there is such a large amount of aggregates.[27,72] For that reason, and even though the used DPI might not be the most appropriate, the

high existence of aggregates is the factor that mainly influences the aerodynamic results because the diminishing of agglomerates was accompanied with the improvement of both FPF and MMAD.

The obtained yields can also be considered small (39% for BSA/leu and 58% for dendrimer/chol formulations), but this can be justified by the inefficient recovery of smaller and lighter particles that were exhausted by the gas flow and also by the small volumes used in each assay, that allows greater loss of particles throughout the apparatus.[102] This is supported with the increase of yield with the formulations with dendrimers that were micronized from an initial solution of higher volume when compared with BSA-loaded PLGA microparticles.

As for the physical-chemical properties of the microparticles, the results obtained from XRD and DSC give similar information. When encapsulating BSA, there is no trace of its original peaks, indicating its total encapsulation and stability. Some of the leucine and cholesterol peaks remain noticed indicating that these compounds do not fully lose their crystalline form. When the dendrimers are encapsulated in PLGA/Chol the resulting powder shows a semi-crystalline state where the broad PLGA peak is noticed. The FTIR analysis confirmed the presence of the compounds by the appearance of characteristic peaks of their functional groups.

From all the pharmacokinetic studies performed there is a biphasic curve for drug release mainly caused by Fickian's diffusion. Drug in contact with the medium, is released as a function of solubility as well as penetration of water into polymer matrix. At this point, there is no appreciable polymer's weight loss and no soluble monomer products are formed. In the second phase, the water inside the matrix slowly hydrolyzes the polymer into soluble monomeric products, creating a passage for the entrapped drug to continue to be released by diffusion.[51]

The biodegradability of the PLGA particles took longer than when the other compounds were present, but still all the formulations took more than a month to stop its degradation. This was already expected since this polymer is known to take approximately two months to fully degrade, being this value dependable on formulation, porosity, surface area and molecular weight.[103] Besides, the existence of aggregates leads to a slower degradation.[104]

The biocompatibility assays confirmed the expected viability of all the formulations, once all the compounds used are known to not have a toxic effect in cells. Moreover, PLGA particles were previously tested for its cytotoxicity in lung cells at several concentrations and all showed closely 100% viability.[105]

5. Conclusion

As presented in the introduction, the development of dry powders for inhalation stands as an outbreak solution to overcome drawbacks associated with drug delivery while the use of sustainable techniques represents a production substitute to surpass the environment issues that affect the industry nowadays. For that, this work represents a research field that has been increasingly growing and taken into consideration worldwide.

Herein, it was proven that the SAA apparatus is capable of producing PLGA dry powder microparticles suitable for inhalation. Throughout the obtained results it is possible to conclude that the particles manufacturing process has associated problems, since it is hard to establish a meeting point between ideal powder properties and SAA parameters. However, with the addition of an API or/and a buking agent those problems can be mildly surpassed.

Overall, by adding both BSA/leucine and SDF-loaded dendrimers/cholesterol to the PLGA particles, these tend to present suitable aerodynamic properties, while maintaining the API stability and preventing its thermal degradation during the production process. The particles showed a controlled release and biodegrability as well as full biocompatibility confirming that PLGA is a good carrier to perform drug delivery to the lungs.

The addition of the bulking agents did increase the suitability of the particles, by helping out reducing the amount of aggregates present in the powder, which was the biggest issue.

It is also possible to conclude that the best obtained formulation for pulmonary vaccine delivery was with BSA/leucine/PLGA, with a MMAD of 2.82 μm, a FPF of 31.73% and a yield of 39%, which present fully proper characteristics for inhalation. As for the treatment of pulmonary hypertension the most appropriate particles were the ones containing the [$Pure_{G4}MeOx$] dendrimer, since they were produced with a yield of 58.23%, with a MMAD of 2.57 μm and a FPF of 36.46%.

Despite that, it would be preferable to proceed with a further particles optimization in order to overcome the problems associated with the aggregation and also the yield, such as the development of a better recovery process in order to avoid such powder loss and the improvement of the formulation with the use of another bulking agent or polymer. It would also be interesting to study macrophage uptake in order to understand if the particles would be able to remain in the lung tissue during the entire drug's release. The next step would be to perform *in vivo* studies to fully understand the microparticles action when inhaled to a living lung.

6. References

1. Takami, T. & Murakami, Y. Development of PEG–PLA/PLGA microparticles for pulmonary drug delivery prepared by a novel emulsification technique assisted with amphiphilic block copolymers. *Colloids Surfaces B Biointerfaces* **87,** 433–438 (2011).

2. Sung, J. C., Pulliam, B. L. & Edwards, D. a. Nanoparticles for drug delivery to the lungs. *Trends Biotechnol.* **25,** 563–70 (2007).

3. Pilcer, G. & Amighi, K. Formulation strategy and use of excipients in pulmonary drug delivery. *Int. J. Pharm.* **392,** 1–19 (2010).

4. Beck-Broichsitter, M. *et al.* Characterization of novel spray-dried polymeric particles for controlled pulmonary drug delivery. *J. Control. Release* **158,** 329–35 (2012).

5. Koushik, K. & Kompella, U. B. Preparation of large porous deslorelin-PLGA microparticles with reduced residual solvent and cellular uptake using a supercritical carbon dioxide process. *Pharm. Res.* **21,** 524–35 (2004).

6. Geiser, M. *et al.* Cellular uptake and localization of inhaled gold nanoparticles in lungs of mice with chronic obstructive pulmonary disease. *Part. Fibre Toxicol.* **10,** 19 (2013).

7. Buttini, F., Colombo, P., Rossi, A., Sonvico, F. & Colombo, G. Particles and powders: tools of innovation for non-invasive drug administration. *J. Control. Release* **161,** 693–702 (2012).

8. Mundargi, R. C., Babu, V. R., Rangaswamy, V., Patel, P. & Aminabhavi, T. M. Nano/micro technologies for delivering macromolecular therapeutics using poly(D,L-lactide-co-glycolide) and its derivatives. *J. Control. Release* **125,** 193–209 (2008).

9. Irvine, D. J., Swartz, M. A. & Szeto, G. L. Engineering synthetic vaccines using cues from natural immunity. *Nat. Publ. Gr.* **12,** 978–990 (2013).

10. Koff, W. C. *et al.* Accelerating next-generation vaccine development for global disease prevention. *Science* **340,** 1232910 (2013).

11. Amorij, J.-P. *et al.* Pulmonary delivery of an inulin-stabilized influenza subunit vaccine prepared by spray-freeze drying induces systemic, mucosal humoral as well as cell-mediated immune responses in BALB/c mice. *Vaccine* **25,** 8707–17 (2007).

12. Sou, T. *et al.* New developments in dry powder pulmonary vaccine delivery. *Trends Biotechnol.* **29,** 191–8 (2011).

13. Pulliam, B., Sung, J. C. & Edwards, D. a. Design of nanoparticle-based dry powder pulmonary vaccines. *Expert Opin. Drug Deliv.* **4,** 651–63 (2007).

14. Alpar, H. O., Somavarapu, S., Atuah, K. N. & Bramwell, V. W. Biodegradable mucoadhesive particulates for nasal and pulmonary antigen and DNA delivery. *Adv. Drug Deliv. Rev.* **57,** 411–30 (2005).

15. Kunda, N. K., Somavarapu, S., Gordon, S. B., Hutcheon, G. a & Saleem, I. Y. Nanocarriers targeting dendritic cells for pulmonary vaccine delivery. *Pharm. Res.* **30,** 325–41 (2013).

16. Bivas-Benita, M. *et al.* Pulmonary delivery of DNA encoding Mycobacterium tuberculosis latency antigen Rv1733c associated to PLGA-PEI nanoparticles enhances T cell responses in a DNA prime/protein boost vaccination regimen in mice. *Vaccine* **27,** 4010–7 (2009).

17. De Swart, R. L. *et al.* Measles vaccination of macaques by dry powder inhalation. *Vaccine* **25,** 1183–90 (2007).

18. Muttil, P. *et al.* Immunization of guinea pigs with novel hepatitis B antigen as nanoparticle aggregate powders administered by the pulmonary route. *AAPS J.* **12,** 330–7 (2010).

19. Yang, J. *et al.* Sildenafil potentiates bone morphogenetic protein signaling in pulmonary arterial smooth muscle cells and in experimental pulmonary hypertension. *Arterioscler. Thromb. Vasc. Biol.* **33,** 34–42 (2013).

20. Archer, S. L. & Michelakis, E. D. Phosphodiesterase type 5 inhibitors for pulmonary arterial hypertension. *N. Engl. J. Med.* **361,** 1864–71 (2009).

21. Baradia, D., Khatri, N., Trehan, S. & Misra, A. Inhalation therapy to treat pulmonary arterial hypertension. *Pharm. Pat. Anal.* **5,** 577–588 (2012).

22. Spring, R. M. *et al.* Sildenafil for pulmonary hypertension: dose-dependent improvement in exercise performance. *Pulm. Pharmacol. Ther.* **21,** 516–21 (2008).

23. Ladha, F. *et al.* Sildenafil improves alveolar growth and pulmonary hypertension in hyperoxia-induced lung injury. *Am. J. Respir. Crit. Care Med.* **172,** 750–6 (2005).

24. Kukowska-Latallo, J. F. *et al.* Intravascular and endobronchial DNA delivery to murine lung tissue using a novel, nonviral vector. *Hum. Gene Ther.* **11,** 1385–95 (2000).

25. Mansour, H. M., Rhee, Y.-S. & Wu, X. Nanomedicine in pulmonary delivery. *Int. J. Nanomedicine* **4,** 299–319 (2009).

26. Restani, R. B. *et al.* Biocompatible polyurea dendrimers with pH-dependent fluorescence. *Angew. Chem. Int. Ed. Engl.* **51,** 5162–5 (2012).

27. Sivadas, N. *et al.* A comparative study of a range of polymeric microspheres as potential carriers for the inhalation of proteins. *Int. J. Pharm.* **358,** 159–67 (2008).

28. Newman, S. P. & Busse, W. W. Evolution of dry powder inhaler design, formulation, and performance. *Respir. Med.* **96,** 293–304 (2002).

29. Shoyele, S. a & Slowey, A. Prospects of formulating proteins/peptides as aerosols for pulmonary drug delivery. *Int. J. Pharm.* **314,** 1–8 (2006).

30. Telko, M. J. & Dsc, A. J. H. Dry Powder Inhaler Formulation. 1209–1227 (2005).

31. Malcolmson, R. J. & Embleton, J. K. Dry powder formulations for pulmonary delivery. *Pharm. Sci. Technolo. Today* **1,** 394–398 (1998).

32. Symbicort, http://www.drugs.com/pro/symbicort.html, Accessed at 20th of July 2014.

33. MIAT, Monodose Inhaler, http://www.miat.it/en/monodose_inhaler.php, Acessed at 20th of July 2014.

34. Choi, H. S. *et al.* Rapid translocation of nanoparticles from the lung airspaces to the body. *Nat. Biotechnol.* **28,** 1300–3 (2010).

35. Hu, J., Dong, Y., Pastorin, G., Ng, W. K. & Tan, R. B. H. Spherical agglomerates of pure drug nanoparticles for improved pulmonary delivery in dry powder inhalers. *J. Nanoparticle Res.* **15,** 1560 (2013).

36. Wanakule, P., Liu, G. W., Fleury, A. T. & Roy, K. Nano-inside-micro: Disease-responsive microgels with encapsulated nanoparticles for intracellular drug delivery to the deep lung. *J. Control. Release* **162,** 429–37 (2012).

37. Li, Y.-Z. *et al.* Inhalable microparticles as carriers for pulmonary delivery of thymopentin-loaded solid lipid nanoparticles. *Pharm. Res.* **27,** 1977–86 (2010).

38. Yang, Y. *et al.* Development of highly porous large PLGA microparticles for pulmonary drug delivery. *Biomaterials* **30,** 1947–53 (2009).

39. Ungaro, F., d'Angelo, I., Miro, A., La Rotonda, M. I. & Quaglia, F. Engineered PLGA nano- and micro-carriers for pulmonary delivery: challenges and promises. *J. Pharm. Pharmacol.* **64,** 1217–35 (2012).

40. Bosquillon, C., Lombry, C., Préat, V. & Vanbever, R. Influence of formulation excipients and physical characteristics of inhalation dry powders on their aerosolization performance. *J. Control. Release* **70,** 329–39 (2001).

41. 2.9.18 Preparations for Inhalation: Aerodynamic Assessment of Fine Particles. European Pharmacopeia 7.0. *Counc. Eur.* 274–285 (2010).

42. <601> Aerosols, Nasal Sprays, Metered-Dose Inhalers, and Dry Powder Inhalers. *U.S. Pharmacop. Natl. Formul. United States Pharmacop. Covention* 46 (2012).

43. Roberts, D. L. & Mitchell, J. P. The effect of nonideal cascade impactor stage collection efficiency curves on the interpretation of the size of inhaler-generated aerosols. *AAPS PharmSciTech* **14,** 497–510 (2013).

44. Mitchell, J. P. *et al.* Relative precision of inhaler aerodynamic particle size distribution (APSD) metrics by full resolution and abbreviated andersen cascade impactors (ACIs): part 1. *AAPS PharmSciTech* **11,** 843–51 (2010).

45. Arifin, D. Y., Lee, L. Y. & Wang, C.-H. Mathematical modeling and simulation of drug release from microspheres: Implications to drug delivery systems. *Adv. Drug Deliv. Rev.* **58,** 1274–325 (2006).

46. Ritger, P. L. & Peppas, N. A. A simple equation for description of solute release. **5,** 23–36 (1987).

47. Lafayette, W. A simple equation for the description of solute release. III. Coupling of diffusion and relaxation. **57,** 169–172 (1989).

48. Pasquali, I., Bettini, R. & Giordano, F. Solid-state chemistry and particle engineering with supercritical fluids in pharmaceutics. *Eur. J. Pharm. Sci.* **27,** 299–310 (2006).

49. Hickey, A. J. *et al.* Physical Characterization of Component Particles Included in Dry Powder Inhalers . I . Strategy Review and Static Characteristics. **96,** 1282–1301 (2007).

50. Lewicki, P. & Hill, T. Statistics: methods and applications. *Tulsa, OK. Statsoft* (2006).

51. Makadia, H. K. & Siegel, S. J. Poly Lactic-co-Glycolic Acid (PLGA) as Biodegradable Controlled Drug Delivery Carrier. *Polymers (Basel).* **3,** 1377–1397 (2011).

52. Cruz, L. J. *et al.* Targeted PLGA nano- but not microparticles specifically deliver antigen to human dendritic cells via DC-SIGN in vitro. *J. Control. Release* **144,** 118–26 (2010).

53. Ibrišimović, N., Al-Dubai, H. & Kerleta, V. Quantification of biodegradable PLGA nanoparticles for drug targeting. *Acta Med. Acad.* (2010).

54. Ding, A. G. & Schwendeman, S. P. Determination of water-soluble acid distribution in poly(lactide-co-glycolide). *J. Pharm. Sci.* **93,** 322–31 (2004).

55. Wade, A. & Weller, P. *Handbook of Pharmaceutical Excipients.* 23–27 (Pharmaceutical Press, 2009).

56. Casettari, L. *et al.* Surface characterisation of bioadhesive PLGA/chitosan microparticles produced by supercritical fluid technology. *Pharm. Res.* **28,** 1668–82 (2011).

57. Nicolete, R., dos Santos, D. F. & Faccioli, L. H. The uptake of PLGA micro or nanoparticles by macrophages provokes distinct in vitro inflammatory response. *Int. Immunopharmacol.* **11,** 1557–63 (2011).

58. Roberts, R. a *et al.* Analysis of the murine immune response to pulmonary delivery of precisely fabricated nano- and microscale particles. *PLoS One* **8,** e62115 (2013).

59. Ungaro, F. *et al.* Dry powders based on PLGA nanoparticles for pulmonary delivery of antibiotics: Modulation of encapsulation efficiency, release rate and lung deposition pattern by hydrophilic polymers. *J. Control. Release* **157,** 149–59 (2012).

60. Wang, C. & Hickey, A. J. Isoxyl aerosols for tuberculosis treatment: preparation and characterization of particles. *AAPS PharmSciTech* **11,** 538–49 (2010).

61. Rehman, M. *et al.* Optimisation of powders for pulmonary delivery using supercritical fluid technology. *Eur. J. Pharm. Sci.* **22,** 1–17 (2004).

62. Vehring, R. Pharmaceutical particle engineering via spray drying. *Pharm. Res.* **25,** 999–1022 (2008).

63. Pilcer, G. & Amighi, K. Formulation strategy and use of excipients in pulmonary drug delivery. *Int. J. Pharm.* **392,** 1–19 (2010).

64. Bisgaard, H., O'Callaghan, C. & Smaldone, G. *Drug delivery to the lung*. *Lung* (2001).

65. Zhang, J., Wu, L., Chan, H.-K. & Watanabe, W. Formation, characterization, and fate of inhaled drug nanoparticles. *Adv. Drug Deliv. Rev.* **63,** 441–55 (2011).

66. Gil, M., Vicente, J. & Gaspar, F. Scale-up methodology for pharmaceutical spray drying. **28,** 18–22 (2010).

67. Street, M. Parmaceutical Spray Drying - Technology Overview and Application in the Pharmaceutical and Biotechnology Industry. *Upperton* 1–7

68. Nie, H., Lee, L. Y., Tong, H. & Wang, C.-H. PLGA/chitosan composites from a combination of spray drying and supercritical fluid foaming techniques: new carriers for DNA delivery. *J. Control. Release* **129,** 207–14 (2008).

69. Tong, H. H. Y. & Chow, A. H. L. Control of Physical Forms of Drug Particles for Pulmonar y Deliver y by Spray Dr ying and Supercritical Fluid Processing. **24,** 27–40 (2006).

70. Barroso, T., Temtem, M., Casimiro, T. & Aguiar-Ricardo, A. Development of pH-responsive poly(methylmethacrylate-co-methacrylic acid) membranes using scCO2 technology. Application to protein permeation. *J. Supercrit. Fluids* **51,** 57–66 (2009).

71. Beckman, E. J. Supercritical and near-critical CO2 in green chemical synthesis and processing. *J. Supercrit. Fluids* **28,** 121–191 (2004).

72. Chow, A. H. L., Tong, H. H. Y., Chattopadhyay, P. & Shekunov, B. Y. Particle engineering for pulmonary drug delivery. *Pharm. Res.* **24,** 411–37 (2007).

73. W, L. & PG, J. in *Handb. Green Chem.* 1–30 (Weihheim: Wiley-VCH, 2010).

74. Chattopadhyay, P. & Gupta, R. B. Supercritical CO 2 Based Production of Magnetically Responsive Micro- and Nanoparticles for Drug Targeting. 6049–6058 (2002).

75. Reverchon, E., Caputo, G. & De Marco, I. Role of Phase Behavior and Atomization in the Supercritical Antisolvent Precipitation. *Ind. Eng. Chem. Res.* **42,** 6406–6414 (2003).

76. Tu, M. Formation of small organic particles by RESS : experimental and theoretical investigations. **15,** 79–89 (1999).

77. Martín, Á., Pham, H. M., Kilzer, A., Kareth, S. & Weidner, E. Micronization of polyethylene glycol by PGSS (Particles from Gas Saturated Solutions)-drying of aqueous solutions. *Chem. Eng. Process. Process Intensif.* **49,** 1259–1266 (2010).

78. Martín, Á. & Weidner, E. PGSS-drying: Mechanisms and modeling. *J. Supercrit. Fluids* **55,** 271–281 (2010).

79. Reverchon, E. Process for the production of micro and/or nano particles. (2007).

80. Reverchon, E., Adami, R. & Caputo, G. Supercritical assisted atomization: Performance comparison between laboratory and pilot scale. *J. Supercrit. Fluids* **37,** 298–306 (2006).

81. Porta, G. Della & Reverchon, E. Engineering Powder Properties By Supercritical Fluid for Optimum Drug Delivery. *Bioprocess Int.* (2005).

82. Reverchon, E. & Antonacci, A. Chitosan Microparticles Production by Supercritical Fluid Processing. *Ind. Eng. Chem. Res.* **45,** 5722–5728 (2006).

83. Reighard, T. S., Lee, S. T. & Olesik, S. V. Determination of methanol/CO2 and acetonitrile/CO2 vapor-liquid phase equilibria using a variable-volume view cell. **vi,** 215–230 (1996).

84. Seju, U., Kumar, a & Sawant, K. K. Development and evaluation of olanzapine-loaded PLGA nanoparticles for nose-to-brain delivery: in vitro and in vivo studies. *Acta Biomater.* **7,** 4169–76 (2011).

85. Azizi, M. *et al.* Fabrication of protein-loaded PLGA nanoparticles: effect of selected formulation variables on particle size and release profile. *J. Polym. Res.* **20,** 110 (2013).

86. Biondi, M., Guarnieri, D., Yu, H., Belli, V. & Netti, P. A. Sub-100 nm biodegradable nanoparticles: in vitro release features and toxicity testing in 2D and 3D cell cultures. *Nanotechnology* **24,** 045101 (2013).

87. Armentano, I., Dottori, M., Puglia, D. & Kenny, J. M. Effects of carbon nanotubes (CNTs) on the processing and in-vitro degradation of poly(DL-lactide-co-glycolide)/CNT films. *J. Mater. Sci. Mater. Med.* **19,** 2377–87 (2008).

88. Marques, M. R. C., Loebenberg, R. & Almukainzi, M. Simulated Biological Fluids with Possible Application in Dissolution Testing. 15–28 (2011).

89. Porta, G. & Adami, R. Albumin/gentamicin microspheres produced by supercritical assisted atomization: optimization of size, drug loading and release. *J. Pharm. Sci.* **99,** 4720–9 (2010).

90. Najafabadi, A. R., Gilani, K., Barghi, M. & Rafiee-Tehrani, M. The effect of vehicle on physical properties and aerosolisation behaviour of disodium cromoglycate microparticles spray dried alone or with L-leucine. *Int. J. Pharm.* **285,** 97–108 (2004).

91. Moghaddam, P. H. *et al.* Development of a nano–micro carrier system for sustained pulmonary delivery of clarithromycin. *Powder Technol.* **239,** 478–483 (2013).

92. Michnik, A. THERMAL STABILITY OF BOVINE SERUM ALBUMIN DSC study. **71,** 509–519 (2003).

93. V, E. S. P. B., Rodante, F. & Marrosu, G. Thermal analysis of some alfa-amino acids using simultaneous Tg-DSC apparatus. The use of dynamic thermogravimetry to study the chemical kinetics of solid state decomposition. *thermichimica Acta* **171,** 15–29 (1990).

94. Kumar, S. Vibrational Spectroscopy Spectroscopic studies of valine and leucine molecules a comparative study. **39,** 4996–4999 (2011).

95. Rehman, M. *et al.* Optimisation of powders for pulmonary delivery using supercritical fluid technology. *Eur. J. Pharm. Sci.* **22,** 1–17 (2004).

96. Fang, D.-L. *et al.* Development of lipid-shell and polymer core nanoparticles with water-soluble salidroside for anti-cancer therapy. *Int. J. Mol. Sci.* **15,** 3373–88 (2014).

97. Zolnik, B. S. & Burgess, D. J. Effect of acidic pH on PLGA microsphere degradation and release. *J. Control. Release* **122,** 338–44 (2007).

98. Edwards, D. a *et al.* Large porous particles for pulmonary drug delivery. *Science* **276,** 1868–71 (1997).

99. Philip, V. a, Mehta, R. C. & DeLuca, P. P. In vitro and in vivo respirable fractions of isopropanol treated PLGA microspheres using a dry powder inhaler. *Int. J. Pharm.* **151,** 175–182 (1997).

100. Rogueda, P. & Traini, D. The nanoscale in pulmonary delivery . Part 2: formulation platform. 607–620 (2007).

101. Philip, V. A., Mehta, R. C., Mazumder, M. K. & Deluca, P. P. Effect of surface treatment on the respirable fractions of PLGA microspheres formulated for dry powder inhalers 1. **151,** 165–174 (1997).

102. Giunchedi, P., Conti, B., Genta, I., Conte, U. & Puglisi, G. Emulsion Spray-Drying for the Preparation of Albumin-Loaded PLGA Microspheres. **27,** 745–750 (2001).

103. Lima, K. M. & Rodrigues Júnior, J. M. Poly-DL-lactide-co-glycolide microspheres as a controlled release antigen delivery system. *Braz. J. Med. Biol. Res.* **32,** 171–80 (1999).

104. Panyam, J. *et al.* Polymer degradation and in vitro release of a model protein from poly(D,L-lactide-co-glycolide) nano- and microparticles. *J. Control. Release* **92,** 173–87 (2003).

105. Zou, W., Liu, C., Chen, Z. & Zhang, N. Studies on bioadhesive PLGA nanoparticles: A promising gene delivery system for efficient gene therapy to lung cancer. *Int. J. Pharm.* **370,** 187–95 (2009).